CHAPTER 40

FLUID MECHANICS

Reuben M. Olson
College of Engineering and Technology
Ohio University
Athens, Ohio

All figures and tables produced, with permission, from *Essentials of Engineering Fluid Mechanics*, Fourth Edition, by Reuben M. Olsen, copyright 1980, Harper & Row, Publishers.

Mechanical Engineers' Handbook, 2nd ed., Edited by Myer Kutz.
ISBN 0-471-13007-9

40.1 DEFINITION OF A FLUID

A solid generally has a definite shape; a fluid has a shape determined by its container. Fluids include liquids, gases, and vapors, or mixtures of these. A fluid continuously deforms when shear stresses are present; it cannot sustain shear stresses at rest. This is characteristic of all real fluids, which are viscous. Ideal fluids are nonviscous (and nonexistent), but have been studied in great detail because in many instances viscous effects in real fluids are very small and the fluid acts essentially as a nonviscous fluid. Shear stresses are set up as a result of relative motion between a fluid and its boundaries or between adjacent layers of fluid.

40.2 IMPORTANT FLUID PROPERTIES

Density ρ and surface tension σ are the most important fluid properties for liquids at rest. Density and viscosity μ are significant for all fluids in motion; surface tension and vapor pressure are significant for cavitating liquids; and bulk elastic modulus K is significant for compressible gases at high subsonic, sonic, and supersonic speeds.

Sonic speed in fluids is $c = \sqrt{K/\rho}$. Thus, for water at 15°C, $c = \sqrt{2.18 \times 10^9/999} = 1480$ m/sec. For a mixture of a liquid and gas bubbles at nonresonant frequencies, $c_m = \sqrt{K_m/\rho_m}$, where m refers to the mixture. This becomes

$$c_m = \sqrt{\frac{p_g K_l}{[xK_l + (1 - x)p_g][x\rho_g + (1 - x)\rho_l]}}$$

where the subscript l is for the liquid phase and g is for the gas phase. Thus, for water at 20°C containing 0.1% gas nuclei by volume at atmospheric pressure, $c_m = 312$ m/sec. For a gas or a mixture of gases (such as air), $c = \sqrt{kRT}$, where $k = c_p/c_v$, R is the gas constant, and T is the absolute temperature. For air at 15°C, $c = \sqrt{(1.4)(287.1)(288)} = 340$ m/sec. This sonic property is thus a combination of two properties, density and elastic modulus.

Kinematic viscosity is the ratio of dynamic viscosity and density. In a Newtonian fluid, simple laminar flow in a direction x at a speed of u, the shearing stress parallel to x is $\tau_L = \mu(du/dy) = \rho\nu(du/dy)$, the product of dynamic viscosity and velocity gradient. In the more general case, $\tau_L = \mu(\partial u/\partial y + \partial v/\partial x)$ when there is also a y component of velocity v. In turbulent flows the shear stress resulting from lateral mixing is $\tau_T = -\rho\overline{u'v'}$, a Reynolds stress, where u' and v' are instantaneous and simultaneous departures from mean values $\bar{u}$ and $\bar{v}$. This is also written as $\tau_T = \rho\epsilon(du/dy)$, where ϵ is called the turbulent eddy viscosity or diffusivity, an indirectly measurable flow parameter and not a fluid property. The eddy viscosity may be orders of magnitude larger than the kinematic viscosity. The total shear stress in a turbulent flow is the sum of that from laminar and from turbulent motion: $\tau = \tau_L + \tau_T = \rho(\nu + \epsilon)du/dy$ after Boussinesq.

40.3 FLUID STATICS

The differential equation relating pressure changes dp with elevation changes dz (positive upward parallel to gravity) is $dp = -\rho g\ dz$. For a constant-density liquid, this integrates to $p_2 - p_1 = -\rho g$ $(z_2 - z_1)$ or $\Delta p = \gamma h$, where γ is in N/m^3 and h is in m. Also $(p_1/\gamma) + z_1 = (p_2/\gamma) + z_2$; a constant piezometric head exists in a homogeneous liquid at rest, and since $p_1/\gamma - p_2/\gamma = z_2 - z_1$, a change in pressure head equals the change in potential head. Thus, horizontal planes are at constant pressure when body forces due to gravity act. If body forces are due to uniform linear accelerations or to centrifugal effects in rigid-body rotations, points equidistant below the free liquid surface are all at the same pressure. Dashed lines in Figs. 40.1 and 40.2 are lines of constant pressure.

Pressure differences are the same whether all pressures are expressed as gage pressure or as absolute pressure.

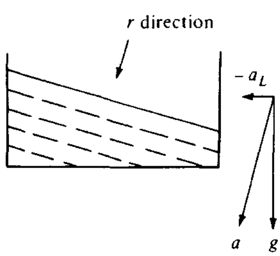

Fig. 40.1 Constant linear acceleration.

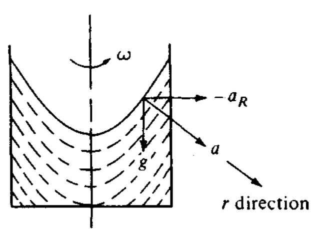

Fig. 40.2 Constant centrifugal acceleration.

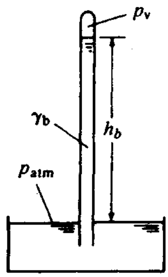

Fig. 40.3 Barometer.

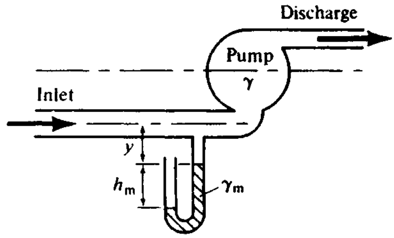

Fig. 40.4 Open manometer.

40.3.1 Manometers

Pressure differences measured by barometers and manometers may be determined from the relation $\Delta p = \gamma h$. In a barometer, Fig. 40.3, $h_b = (p_a - p_v)/\gamma_b$ m.

An open manometer, Fig. 40.4, indicates the inlet pressure for a pump by $p_{\text{inlet}} = -\gamma_m h_m - \gamma y$ Pa gage. A differential manometer, Fig. 40.5, indicates the pressure drop across an orifice, for example, by $p_1 - p_2 = h_m(\gamma_m - \gamma_0)$ Pa.

Manometers shown in Figs. 40.3 and 40.4 are a type used to measure medium or large pressure differences with relatively small manometer deflections. Micromanometers can be designed to produce relatively large manometer deflections for very small pressure differences. The relation $\Delta p = \gamma \Delta h$ may be applied to the many commercial instruments available to obtain pressure differences from the manometer deflections.

40.3.2 Liquid Forces on Submerged Surfaces

The liquid force on any flat surface submerged in the liquid equals the product of the gage pressure at the centroid of the surface and the surface area, or $F = \bar{p}A$. The force F is not applied at the centroid for an inclined surface, but is always below it by an amount that diminishes with depth. Measured parallel to the inclined surface, $\bar{y}$ is the distance from 0 in Fig. 40.6 to the centroid and $y_F = \bar{y} + I_{CG}/A\bar{y}$, where I_{CG} is the moment of inertia of the flat surface with respect to its centroid. Values for some surfaces are listed in Table 40.1.

For curved surfaces, the horizontal component of the force is equal in magnitude and point of application to the force on a projection of the curved surface on a vertical plane, determined as above. The vertical component of force equals the weight of liquid above the curved surface and is applied at the centroid of this liquid, as in Fig. 40.7. The liquid forces on opposite sides of a submerged surface are equal in magnitude but opposite in direction. These statements for curved surfaces are also valid for flat surfaces.

Buoyancy is the resultant of the surface forces on a submerged body and equals the weight of fluid (liquid or gas) displaced.

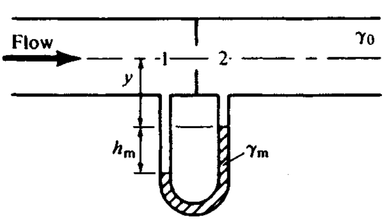

Fig. 40.5 Differential manometer.

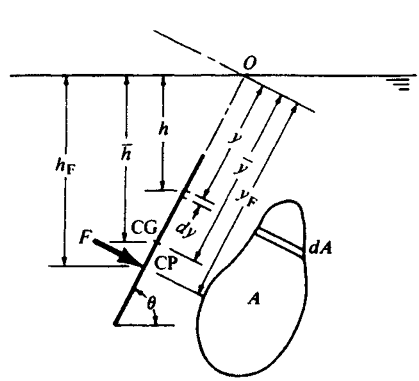

Fig. 40.6 Flat inclined surface submerged in a liquid.

Table 40.1 Moments of Inertia for Various Plane Surfaces about Their Center of Gravity

Surface		I_{CG}
Rectangle or square	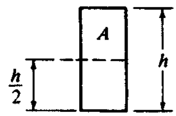	$\frac{1}{12}Ah^2$
Triangle	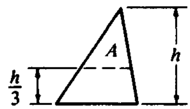	$\frac{1}{18}Ah^2$
Quadrant of circle (or semicircle)	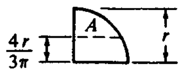	$\left(\frac{1}{4}-\frac{16}{9\pi^2}\right)Ar^2 = 0.0699\ Ar^2$
Quadrant of ellipse (or semiellipse)	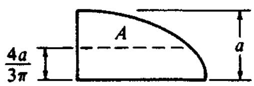	$\left(\frac{1}{4}-\frac{16}{9\pi^2}\right)Aa^2 = 0.0699\ Aa^2$
Parabola	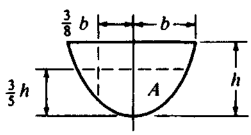	$\left(\frac{3}{7}-\frac{9}{25}\right)Ah^2 = 0.0686\ Ah^2$
Circle	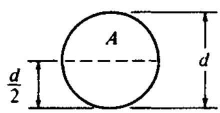	$\frac{1}{16}Ad^2$
Ellipse	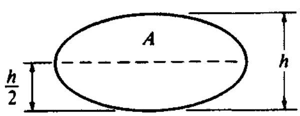	$\frac{1}{16}Ah^2$

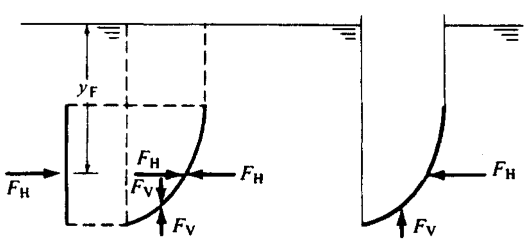

Fig. 40.7 Curved surfaces submerged in a liquid.

40.3.3 Aerostatics

The U.S. standard atmosphere is considered to be dry air and to be a perfect gas. It is defined in terms of the temperature variation with altitude (Fig. 40.8), and consists of isothermal regions and polytropic regions in which the polytropic exponent n depends on the lapse rate (temperature gradient).

Conditions at an upper altitude z_2 and at a lower one z_1 in an isothermal atmosphere are obtained by integrating the expression $dp = -\rho g\, dz$ to get

$$\frac{p_2}{p_1} = \exp \frac{-g(z_2 - z_1)}{RT}$$

In a polytropic atmosphere where $p/p_1 = (\rho/\rho_1)^n$,

$$\frac{p_2}{p_1} = \left[1 - g\frac{(n-1)}{n}\frac{(z_2 - z_1)}{RT_1}\right]^{n/(n-1)}$$

from which the lapse rate is $(T_2 - T_1)/(z_2 - z_1) = -g(n-1)/nR$ and thus n is obtained from $1/n = 1 + (R/g)(dt/dz)$. Defining properties of the U.S. standard atmosphere are listed in Table 40.2.

The U.S. standard atmosphere is used in measuring altitudes with altimeters (pressure gages) and, because the altimeters themselves do not account for variations in the air temperature beneath an aircraft, they read too high in cold weather and too low in warm weather.

40.3.4 Static Stability

For the *atmosphere* at rest, if an air mass moves very slowly vertically and remains there, the atmosphere is neutral. If vertical motion continues, it is unstable; if the air mass moves to return to its initial position, it is stable. It can be shown that atmospheric stability may be defined in terms of the polytropic exponent. If $n < k$, the atmosphere is stable (see Table 40.2); if $n = k$, it is neutral (adiabatic); and if $n > k$, it is unstable.

The stability of a body *submerged* in a fluid at rest depends on its response to forces which tend to tip it. If it returns to its original position, it is stable; if it continues to tip, it is unstable; and if it remains at rest in its tipped position, it is neutral. In Fig. 40.9 G is the center of gravity and B is the center of buoyancy. If the body in (a) is tipped to the position in (b), a couple Wd restores the body toward position (a) and thus the body is stable. If B were below G and the body displaced, it would move until B becomes above G. Thus stability requires that G is below B.

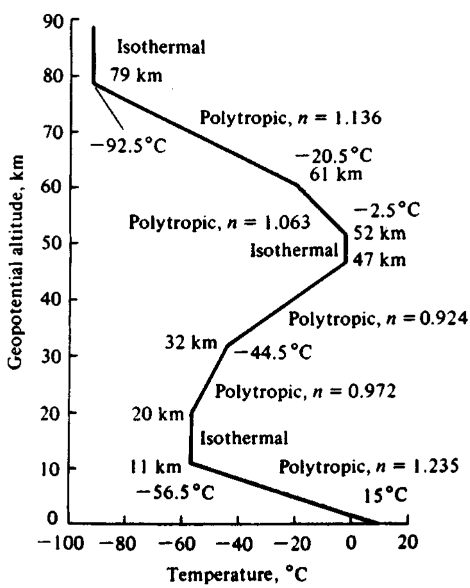

Fig. 40.8 U.S. standard atmosphere.

Table 40.2 Defining Properties of the U.S. Standard Atmosphere

Altitude (m)	Temperature (°C)	Type of Atmosphere	Lapse Rate (°C/km)	$\bar{g}$ (m/s²)	n	Pressure p(Pa)	Density ρ(kg/m³)
0	15.0					1.013×10^5	1.225
		Polytropic	−6.5	9.790	1.235		
11,000	−56.5					2.263×10^4	3.639×10^{-1}
		Isothermal	0.0	9.759			
20,000	−56.5					5.475×10^3	8.804×10^{-2}
		Polytropic	+1.0	9.727	0.972		
32,000	−44.5					8.680×10^2	1.323×10^{-2}
		Polytropic	+2.8	9.685	0.924		
47,000	−2.5					1.109×10^2	1.427×10^{-3}
		Isothermal	0.0	9.654			
52,000	−2.5					5.900×10^1	7.594×10^{-4}
		Polytropic	−2.0	9.633	1.063		
61,000	−20.5					1.821×10^1	2.511×10^{-4}
		Polytropic	−4.0	9.592	1.136		
79,000	−92.5					1.038	2.001×10^{-5}
		Isothermal	0.0	9.549			
88,743	−92.5					1.644×10^{-1}	3.170×10^{-6}

Floating bodies may be stable even though the center of buoyancy B is below the center of gravity G. The center of buoyancy generally changes position when a floating body tips because of the changing shape of the displaced liquid. The floating body is in equilibrium in Fig. 40.10*a*. In Fig. 40.10*b* the center of buoyancy is at B_1, and the restoring couple rotates the body toward its initial position in Fig. 40.10*a*. The intersection of BG is extended and a vertical line through B_1 is at M, the metacenter, and GM is the metacentric height. The body is stable if M is above G. Thus, the position of B relative to G determines stability of a submerged body, and the position of M relative to G determines the stability of floating bodies.

40.4 FLUID KINEMATICS

Fluid flows are classified in many ways. Flow is *steady* if conditions at a point do not vary with time, or for turbulent flow, if mean flow parameters do not vary with time. Otherwise the flow is *unsteady.* Flow is considered *one dimensional* if flow parameters are considered constant throughout a cross section, and variations occur only in the flow direction. *Two-dimensional* flow is the same in parallel planes and is not one dimensional. In *three-dimensional* flow gradients of flow parameters exist in three mutually perpendicular directions (x, y, and z). Flow may be *rotational* or *irrotational,* depending on whether the fluid particles rotate about their own centers or not. Flow is *uniform* if the velocity does not change in the direction of flow. If it does, the flow is *nonuniform. Laminar* flow exists when there are no lateral motions superimposed on the mean flow. When there are, the flow is *turbulent.* Flow may be intermittently laminar and turbulent; this is called flow in *transition.* Flow is considered *incompressible* if the density is constant, or in the case of gas flows, if the density

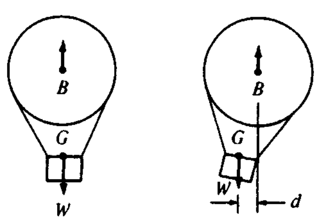

(*a*) (*b*)

Fig. 40.9 Stability of a submerged body.

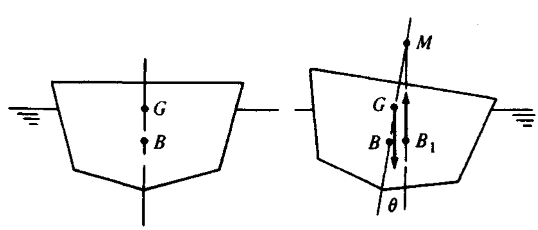

(*a*) (*b*)

Fig. 40.10 Floating body.

variation is below a specified amount throughout the flow, 2–3%, for example. Low-speed gas flows may be considered essentially incompressible. Gas flows may be considered as *subsonic, transonic, sonic, supersonic,* or *hypersonic* depending on the gas speed compared with the speed of sound in the gas. Open-channel water flows may be designated as *subcritical, critical,* or *supercritical* depending on whether the flow is less than, equal to, or greater than the speed of an elementary surface wave.

40.4.1 Velocity and Acceleration

In Cartesian coordinates, velocity components are u, v, and w in the x, y, and z directions, respectively. These may vary with position and time, such that, for example, $u = dx/dt = u(x, y, z, t)$. Then

$$du = \frac{\partial u}{\partial x}dx + \frac{\partial u}{\partial y}dy + \frac{\partial u}{\partial z}dz + \frac{\partial u}{\partial t}dt$$

and

$$\begin{aligned} a_x &= \frac{du}{dt} = \frac{\partial u}{\partial x}\frac{dx}{dt} + \frac{\partial u}{\partial y}\frac{dy}{dt} + \frac{\partial u}{\partial z}\frac{dz}{dt} + \frac{\partial u}{\partial t} \\ &= \frac{Du}{Dt} = u\frac{\partial u}{\partial x} + v\frac{\partial u}{\partial y} + w\frac{\partial u}{\partial z} + \frac{\partial u}{\partial t} \end{aligned}$$

The first three terms on the right hand side are the *convective* acceleration, which is zero for uniform flow, and the last term is the *local* acceleration, which is zero for steady flow.

In natural coordinates (streamline direction s, normal direction n, and meridional direction m normal to the plane of s and n), the velocity V is always in the streamline direction. Thus, $V = V(s,t)$ and

$$dV = \frac{\partial V}{\partial s}ds + \frac{\partial V}{\partial t}dt$$

$$a_s = \frac{dV}{dt} = V\frac{\partial V}{\partial s} + \frac{\partial V}{\partial t}$$

where the first term on the right-hand side is the *convective* acceleration and the last is the *local* acceleration. Thus, if the fluid velocity changes as the fluid moves throughout space, there is a convective acceleration, and if the velocity at a point changes with time, there is a local acceleration.

40.4.2 Streamlines

A *streamline* is a line to which, at each instant, velocity vectors are tangent. A *pathline* is the path of a particle as it moves in the fluid, and for steady flow it coincides with a streamline.

The equations of streamlines are described by stream functions ψ, from which the velocity components in two-dimensional flow are $u = -\partial\psi/\partial y$ and $v = +\partial\psi/\partial x$. Streamlines are lines of constant stream function. In polar coordinates

$$v_r = -\frac{1}{r}\frac{\partial\psi}{\partial\theta} \quad \text{and} \quad v_\theta = +\frac{\partial\psi}{\partial r}$$

Some streamline patterns are shown in Figs. 40.11, 40.12, and 40.13. The lines at right angles to the streamlines are potential lines.

40.4.3 Deformation of a Fluid Element

Four types of deformation or movement may occur as a result of spatial variations of velocity: translation, linear deformation, angular deformation, and rotation. These may occur singly or in combination. Motion of the face (in the x-y plane) of an elemental cube of sides δx, δy, and δz in a time dt is shown in Fig. 40.14. Both translation and rotation involve motion or deformation without a change in shape of the fluid element. Linear and angular deformations, however, do involve a change in shape of the fluid element. Only through these linear and angular deformations are heat generated and mechanical energy dissipated as a result of viscous action in a fluid.

For linear deformation the relative change in volume is at a rate of

$$(\mathcal{V}_{dt} - \mathcal{V}_0)/\mathcal{V}_0 = \frac{\partial u}{\partial x} + \frac{\partial v}{\partial y} + \frac{\partial w}{\partial z} = \text{div V}$$

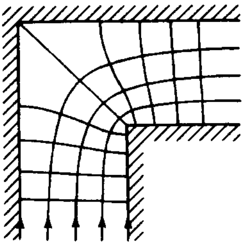

Fig. 40.11 Flow around a corner in a duct.

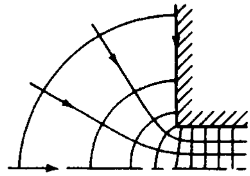

Fig. 40.12 Flow around a corner into a duct.

which is zero for an incompressible fluid, and thus is an expression for the continuity equation. Rotation of the face of the cube shown in Fig. 40.14*d* is the average of the rotations of the bottom and left edges, which is

$$\frac{1}{2}\left(\frac{\partial v}{\partial x} - \frac{\partial u}{\partial y}\right) dt$$

The rate of rotation is the angular velocity and is

$$\omega_z = \frac{1}{2}\left(\frac{\partial v}{\partial x} - \frac{\partial u}{\partial y}\right) \quad \text{about the } z \text{ axis in the } x\text{-}y \text{ plane}$$

$$\omega_x = \frac{1}{2}\left(\frac{\partial w}{\partial y} - \frac{\partial v}{\partial z}\right) \quad \text{about the } x \text{ axis in the } y\text{-}z \text{ plane}$$

and

$$\omega_y = \frac{1}{2}\left(\frac{\partial u}{\partial z} - \frac{\partial w}{\partial x}\right) \quad \text{about the } y \text{ axis in the } x\text{-}z \text{ plane}$$

These are the components of the angular velocity vector Ω,

$$\Omega = \tfrac{1}{2} \text{ curl V} = \frac{1}{2}\begin{vmatrix} \mathrm{i} & \mathrm{j} & \mathrm{k} \\ \dfrac{\partial}{\partial x} & \dfrac{\partial}{\partial y} & \dfrac{\partial}{\partial z} \\ u & v & w \end{vmatrix} = \omega_x \mathrm{i} + \omega_y \mathrm{j} + \omega_z \mathrm{k}$$

If the flow is irrotational, these quantities are zero.

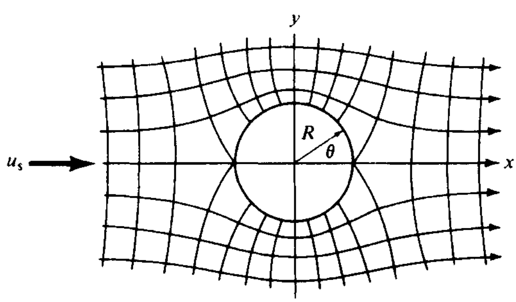

Fig. 40.13 Inviscid flow past a cylinder.

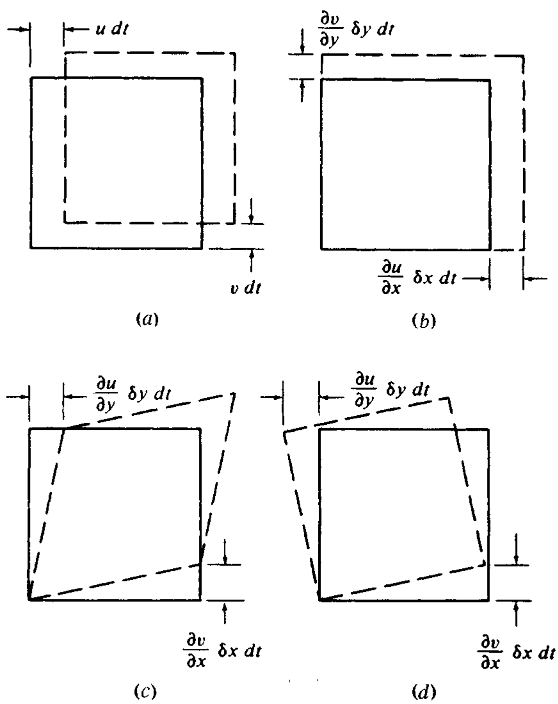

Fig. 40.14 Movements of the face of an elemental cube in the *x*-*y* plane: (*a*) translation; (*b*) linear deformation; (*c*) angular deformation; (*d*) rotation.

40.4.4 Vorticity and Circulation

Vorticity is defined as twice the angular velocity, and thus is also zero for irrotational flow. Circulation is defined as the line integral of the velocity component along a closed curve and equals the total strength of all vertex filaments that pass through the curve. Thus, the vorticity at a point within the curve is the circulation per unit area enclosed by the curve. These statements are expressed by

$$\Gamma = \oint \mathbf{V} \cdot d\mathbf{l} = \oint (u\,dx + v\,dy + w\,dz) \qquad \text{and} \qquad \zeta_A = \lim_{A \to 0} \frac{\Gamma}{A}$$

Circulation—the product of vorticity and area—is the counterpart of volumetric flow rate as the product of velocity and area. These are shown in Fig. 40.15.

Physically, fluid rotation at a point in a fluid is the instantaneous average rotation of two mutually perpendicular infinitesimal line segments. In Fig. 40.16 the line δx rotates positively and δy rotates

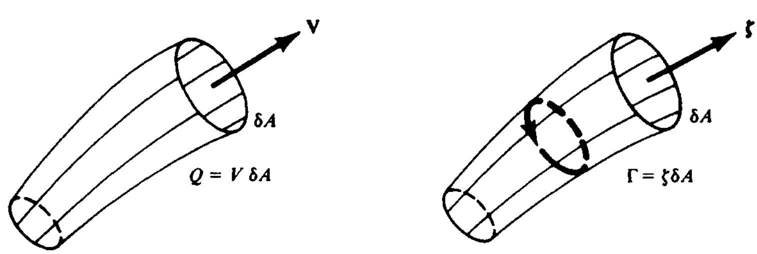

Fig. 40.15 Similarity between a stream filament and a vortex filament.

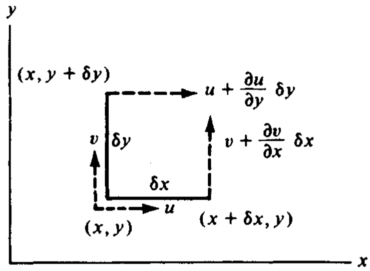

Fig. 40.16 Rotation of two line segments in a fluid.

negatively. Then $\omega_x = (\partial v/\partial x - \partial u/\partial y)/2$. In natural coordinates (the n direction is opposite to the radius of curvature r) the angular velocity in the s-n plane is

$$\omega = \frac{1}{2}\frac{\Gamma}{\delta A} = \frac{1}{2}\left(\frac{V}{r} - \frac{\partial V}{\partial n}\right) = \frac{1}{2}\left(\frac{V}{r} + \frac{\partial V}{\partial r}\right)$$

This shows that for irrotational motion $V/r = \partial V/\partial n$ and thus the peripheral velocity V increases toward the center of curvature of streamlines. In an irrotational vortex, $Vr = C$ and in a solid-body-type or rotational vortex, $V = \omega r$.

A combined vortex has a solid-body-type rotation at the core and an irrotational vortex beyond it. This is typical of a tornado (which has an inward sink flow superimposed on the vortex motion) and eddies in turbulent motion.

40.4.5 Continuity Equations

Conservation of mass for a fluid requires that in a *material* volume, the mass remains constant. In a *control* volume the net rate of influx of mass into the control volume is equal to the rate of change of mass in the control volume. Fluid may flow into a control volume either through the control surface or from internal sources. Likewise, fluid may flow out through the control surface or into internal sinks. The various forms of the continuity equations listed in Table 40.3 do not include sources and sinks; if they exist, they must be included.

The most commonly used forms for duct flow are $\dot{m} = VA\rho$ in kg/sec where V is the average flow velocity in m/sec, A is the duct area in m^3, and ρ is the fluid density in kg/m^3. In differential form this is $dV/V + dA/A + d\rho/\rho = 0$, which indicates that all three quantities may not increase nor all decrease in the direction of flow. For incompressible duct flow $Q = VA$ m^3/sec where V and A are as above. When the velocity varies throughout a cross section, the average velocity is

$$V = \frac{1}{A}\int u dA = \frac{1}{n}\sum_{i=1}^{n} u_i$$

where u is a velocity at a point, and u_i are point velocities measured at the centroid of n equal areas. For example, if the velocity is u at a distance y from the wall of a pipe of radius R and the centerline velocity is u_m, $u = u_m(y/R)^{1/7}$ and the average velocity is $V = {}^{49}\!/\!_{60}\, u_m$.

40.5 FLUID MOMENTUM

The momentum theorem states that the net external force acting on the fluid within a control volume equals the time rate of change of momentum of the fluid plus the net rate of momentum flux or transport out of the control volume through its surface. This is one form of the Reynolds transport theorem, which expresses the conservation laws of physics for fixed mass systems to expressions for a control volume:

$$\begin{aligned}\Sigma\mathbf{F} &= \frac{D}{Dt}\int_{\substack{\text{material}\\\text{volume}}} \rho\mathbf{V}\, d\forall \\ &= \frac{\partial}{\partial t}\int_{\substack{\text{control}\\\text{volume}}} \rho\mathbf{V}\, d\forall + \int_{\substack{\text{control}\\\text{surface}}} \rho\mathbf{V}(\mathbf{V}\cdot d\mathbf{s})\end{aligned}$$

Table 40.3 Continuity Equations

General	$\dfrac{\partial\rho}{\partial t} + \nabla\cdot\rho\mathbf{V} = 0$ or $\dfrac{D\rho}{Dt} + \rho\nabla\cdot\mathbf{V} = 0$	Vector
Unsteady, compressible	$\dfrac{\partial\rho}{\partial t} + \dfrac{\partial(\rho u)}{\partial x} + \dfrac{\partial(\rho v)}{\partial y} + \dfrac{\partial(\rho w)}{\partial z} = 0$	Cartesian
	$\dfrac{\partial\rho}{\partial t} + \dfrac{\partial(\rho v_r)}{\partial r} + \dfrac{1}{r}\dfrac{\partial(\rho v_\theta)}{\partial\theta} + \dfrac{\partial(\rho v_z)}{\partial z} + \dfrac{\rho v_r}{r} = 0$	Cylindrical
	$\dfrac{\partial(\rho A)}{\partial t} + \dfrac{\partial}{\partial s}(\rho\mathbf{V}\cdot\mathbf{A}) = 0$	Duct
Steady, compressible	$\nabla\cdot\rho\mathbf{V} = 0$	Vector
	$\dfrac{\partial(\rho u)}{\partial x} + \dfrac{\partial(\rho v)}{\partial y} + \dfrac{\partial(\rho w)}{\partial z} = 0$	Cartesian
	$\dfrac{\partial(\rho v_r)}{\partial r} + \dfrac{1}{r}\dfrac{\partial(\rho v_\theta)}{\partial\theta} + \dfrac{\partial(\rho v_z)}{\partial z} + \dfrac{\rho v_r}{r} = 0$	Cylindrical
	$\rho\mathbf{V}\cdot\mathbf{A} = \dot{m}$	
Incompressible	$\nabla\cdot\mathbf{V} = 0$	Vector
Steady or unsteady	$\dfrac{\partial u}{\partial x} + \dfrac{\partial v}{\partial y} + \dfrac{\partial w}{\partial z} = 0$	Cartesian
	$\dfrac{\partial v_r}{\partial r} + \dfrac{1}{r}\dfrac{\partial v_\theta}{\partial\theta} + \dfrac{\partial v_z}{\partial z} + \dfrac{v_r}{r} = 0$	Cylindrical
	$\mathbf{V}\cdot\mathbf{A} = Q$	Duct

40.5.1 The Momentum Theorem

For steady flow the first term on the right-hand side of the preceding equation is zero. Forces include normal forces due to pressure and tangential forces due to viscous shear over the surface S of the control volume, and body forces due to gravity and centrifugal effects, for example. In scalar form the net force equals the total momentum flux leaving the control volume minus the total momentum flux entering the control volume. In the x direction

$$\Sigma F_x = (\dot{m}V_x)_{\text{leaving } S} - (\dot{m}V_x)_{\text{entering } S}$$

or when the same fluid enters and leaves,

$$\Sigma F_x = \dot{m}(V_{x\,\text{leaving } S} - V_{x\,\text{entering } S})$$

with similar expressions for the y and z directions.

For one-dimensional flow $\dot{m}V_x$ represents momentum flux passing a section and V_x is the average velocity. If the velocity varies across a duct section, the true momentum flux is $\int_A (u\rho dA)u$, and the ratio of this value to that based upon average velocity is the momentum correction factor β,

$$\beta = \frac{\displaystyle\int_A u^2\,dA}{V^2A} \geq 1$$
$$\approx \frac{1}{V^2n}\sum_{i=1}^{n} u_i^2$$

For laminar flow in a circular tube, $\beta = 4/3$; for laminar flow between parallel plates, $\beta = 1.20$; and for turbulent flow in a circular tube, β is about $1.02 - 1.03$.

40.5.2 Equations of Motion

For steady irrotational flow of an incompressible nonviscous fluid, Newton's second law gives the Euler equation of motion. Along a streamline it is

$$V\frac{\partial V}{\partial s} + \frac{1}{\rho}\frac{\partial p}{\partial s} + g\frac{\partial z}{\partial s} = 0$$

and normal to a streamline it is

$$\frac{V^2}{r} + \frac{1}{\rho}\frac{\partial p}{\partial n} + g\frac{\partial z}{\partial n} = 0$$

When integrated, these show that the sum of the kinetic, displacement, and potential energies is a constant along streamlines as well as across streamlines. The result is known as the Bernoulli equation:

$$\frac{V^2}{2} + \frac{p}{\rho} + gz = \text{constant energy per unit mass}$$

$$\frac{\rho V_1^2}{2} + p_1 + \rho g z_1 = \frac{\rho V_2^2}{2} + p_2 + \rho g z_2 = \text{constant total pressure}$$

and

$$\frac{V_1^2}{2g} + \frac{p_1}{g\rho} + z_1 = \frac{V_2^2}{2g} + \frac{p_2}{g\rho} + z_2 = \text{constant total head}$$

For a reversible adiabatic compressible gas flow with no external work, the Euler equation integrates to

$$\frac{V_1^2}{2} + \frac{k}{k-1}\left(\frac{p_1}{\rho_1}\right) + gz_1 = \frac{V_2^2}{2} + \frac{k}{k-1}\left(\frac{p_2}{\rho_2}\right) + gz_2$$

which is valid whether the flow is reversible or not, and corresponds to the steady-flow energy equation for adiabatic no-work gas flow.

Newton's second law written normal to streamlines shows that in horizontal planes $dp/dr = \rho V^2/r$, and thus dp/dr is positive for both rotational and irrotational flow. The pressure increases away from the center of curvature and decreases toward the center of curvature of curvilinear streamlines. The radius of curvature r of straight lines is infinite, and thus no pressure gradient occurs across these.

For a liquid rotating as a solid body

$$-\frac{V_1^2}{2g} + \frac{p_1}{\rho g} + z_1 = -\frac{V_2^2}{2g} + \frac{p_2}{\rho g} + z_2$$

The negative sign balances the increase in velocity and pressure with radius.

The differential equations of motion for a viscous fluid are known as the Navier–Stokes equations. For incompressible flow the x-component equation is

$$\frac{\partial u}{\partial t} + u\frac{\partial u}{\partial x} + v\frac{\partial u}{\partial y} + w\frac{\partial u}{\partial z} = X - \frac{1}{\rho}\frac{\partial p}{\partial x} + v\left(\frac{\partial^2 u}{\partial x^2} + \frac{\partial^2 u}{\partial y^2} + \frac{\partial^2 u}{\partial z^2}\right)$$

with similar expressions for the y and z directions. X is the body force per unit mass. Reynolds developed a modified form of these equations for turbulent flow by expressing each velocity as an average value plus a fluctuating component ($u = \bar{u} + u'$ and so on). These modified equations indicate shear stresses from turbulence ($\tau_T = -\rho\overline{u'v'}$, for example) known as the Reynolds stresses, which have been useful in the study of turbulent flow.

40.6 FLUID ENERGY

The Reynolds transport theorem for fluid passing through a control volume states that the heat added to the fluid less any work done by the fluid increases the energy content of the fluid in the control volume or changes the energy content of the fluid as it passes through the control surface. This is

$$Q - Wk_{\text{done}} = \frac{\partial}{\partial t}\int_{\substack{\text{control}\\ \text{volume}}} (e\rho)\, d\mathcal{V} + \int_{\substack{\text{control}\\ \text{surface}}} e\rho(\mathbf{V}\cdot d\mathbf{S})$$

and represents the first law of thermodynamics for control volume. The energy content includes kinetic, internal, potential, and displacement energies. Thus, mechanical and thermal energies are included, and there are no restrictions on the direction of interchange from one form to the other implied in the first law. The second law of thermodynamics governs this.

40.6.1 Energy Equations

With reference to Fig. 40.17, the steady flow energy equation is

$$\alpha_1 \frac{V_1^2}{2} + p_1 v_1 + g z_1 + u_1 + q - w = \alpha_2 \frac{V_2^2}{2} + p_2 v_2 + g z_2 + u_2$$

in terms of energy per unit mass, and where α is the kinetic energy correction factor:

$$\alpha = \frac{\int_A u^3\, dA}{V^3 A} \approx \frac{1}{V^3 n} \sum_{i=1}^{n} u_i^3 \geq 1$$

For laminar flow in a pipe, $\alpha = 2$; for turbulent flow in a pipe, $\alpha = 1.05 - 1.06$; and if one-dimensional flow is assumed, $\alpha = 1$.

For one-dimensional flow of compressible gases, the general expression is

$$\frac{V_1^2}{2} + h_1 + g z_1 + q - w = \frac{V_2^2}{2} + h_2 + g z_2$$

For adiabatic flow, $q = 0$; for no external work, $w = 0$; and in most instances changes in elevation z are very small compared with changes in other parameters and can be neglected. Then the equation becomes

$$\frac{V_1^2}{2} + h_1 = \frac{V_2^2}{2} + h_2 = h_0$$

where h_0 is the stagnation enthalpy. The stagnation temperature is then $T_0 = T_1 + V_1^2/2c_p$ in terms of the temperature and velocity at some point 1. The gas velocity in terms of the stagnation and static temperatures, respectively, is $V_1 = \sqrt{2c_p(T_0 - T_1)}$. An increase in velocity is accompanied by a decrease in temperature, and vice versa.

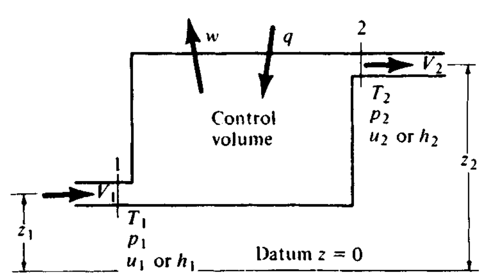

Fig. 40.17 Control volume for steady-flow energy equation.

For one-dimensional flow of liquids and constant-density (low-velocity) gases, the energy equation generally is written in terms of energy per unit weight as

$$\frac{V_1^2}{2g} + \frac{p_1}{\gamma} + z_1 - w = \frac{V_2^2}{2g} + \frac{p_2}{\gamma} + z_2 + h_L$$

where the first three terms are velocity, pressure, and potential heads, respectively. The head loss $h_L = (u_2 - u_1 - q)/g$ and represents the mechanical energy dissipated into thermal energy irreversibly (the heat transfer q is assumed zero here). It is a positive quantity and increases in the direction of flow.

Irreversibility in compressible gas flows results in an entropy increase. In Fig. 40.18 reversible flow between pressures p' and p is from a to b or from b to a. Irreversible flow from p' to p is from b to d, and from p to p' it is from a to c. Thus, frictional duct flow from one pressure to another results in a higher final temperature, and a lower final velocity, in both instances. For frictional flow between given temperatures (T_a and T_b, for example), the resulting pressures are lower than for frictionless flow (p_c is lower than p_a and p_f is lower than p_b).

40.6.2 Work and Power

Power is the rate at which work is done, and is the work done per unit mass times the mass flow rate, or the work done per unit weight times the weight flow rate.

Power represented by the work term in the energy equation is $P = w(VA\gamma) = w(VA\rho)$W.

Power in a jet at a velocity V is $P = (V^2/2)(VA\rho) = (V^2/2g)(VA\gamma)$W.

Power loss resulting from head loss is $P = h_L(VA\gamma)$W.

Power to overcome a drag force is $P = FV$W.

Power available in a hydroelectric power plant when water flows from a headwater elevation z_1 to a tailwater elevation z_2 is $P = (z_1 - z_2)(Q\gamma)$W, where Q is the volumetric flow rate.

40.6.3 Viscous Dissipation

Dissipation effects resulting from viscosity account for entropy increases in adiabatic gas flows and the heat loss term for flows of liquids. They can be expressed in terms of the rate at which work is done—the product of the viscous shear force on the surface of an elemental fluid volume and the corresponding component of velocity parallel to the force. Results for a cube of sides dx, dy, and dz give the dissipation function Φ:

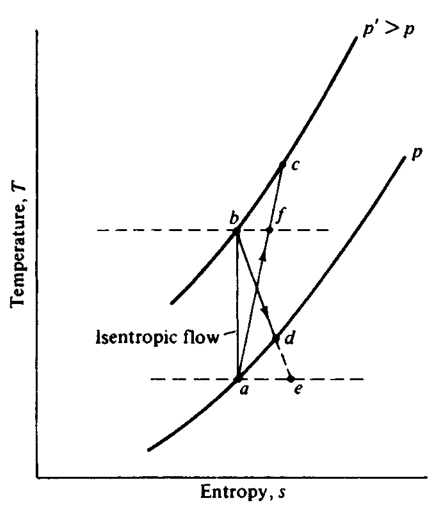

Fig. 40.18 Reversible and irreversible adiabatic flows.

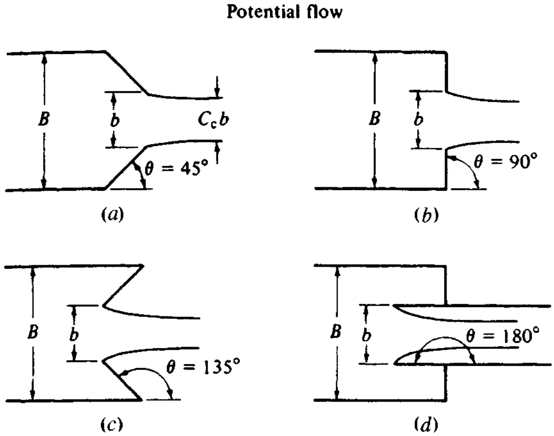

Fig. 40.19 Geometry of two-dimensional jets.

$$\Phi = 2\mu \left[\left(\frac{\partial u}{\partial x}\right)^2 + \left(\frac{\partial v}{\partial y}\right)^2 + \left(\frac{\partial w}{\partial z}\right)^2 \right] + \mu \left[\left(\frac{\partial v}{\partial x} + \frac{\partial u}{\partial y}\right)^2 + \left(\frac{\partial w}{\partial y} + \frac{\partial v}{\partial z}\right)^2 + \left(\frac{\partial u}{\partial z} + \frac{\partial w}{\partial x}\right)^2 \right] - \frac{2}{3}\mu \left(\frac{\partial u}{\partial x} + \frac{\partial v}{\partial y} + \frac{\partial w}{\partial z}\right)^2$$

The last term is zero for an incompressible fluid. The first term in brackets is the linear deformation, and the second term in brackets is the angular deformation and in only these two forms of deformation is there heat generated as a result of viscous shear within the fluid. The second law of thermodynamics precludes the recovery of this heat to increase the mechanical energy of the fluid.

40.7 CONTRACTION COEFFICIENTS FROM POTENTIAL FLOW THEORY

Useful engineering results of a conformal mapping technique were obtained by von Mises for the contraction coefficients of two-dimensional jets for nonviscous incompressible fluids in the absence of gravity. The ratio of the resulting cross-sectional area of the jet to the area of the boundary opening is called the *coefficient of contraction*, C_c. For flow geometries shown in Fig. 40.19, von Mises calculated the values of C_c listed in Table 40.4. The values agree well with measurements for low-viscosity liquids. The results tabulated for two-dimensional flow may be used for axisymmetric jets if C_c is defined by $C_c = b_{jet}/b = (d_{jet}/d)^2$ and if d and D are diameters equivalent to widths b and

Table 40.4 Coefficients of Contraction for Two-Dimensional Jets

b/B	C_c $\theta = 45°$	C_c $\theta = 90°$	C_c $\theta = 135°$	C_c $\theta = 180°$
0.0	0.746	0.611	0.537	0.500
0.1	0.747	0.612	0.546	0.513
0.2	0.747	0.616	0.555	0.528
0.3	0.748	0.622	0.566	0.544
0.4	0.749	0.631	0.580	0.564
0.5	0.752	0.644	0.599	0.586
0.6	0.758	0.662	0.620	0.613
0.7	0.768	0.687	0.652	0.646
0.8	0.789	0.722	0.698	0.691
0.9	0.829	0.781	0.761	0.760
1.0	1.000	1.000	1.000	1.000

B, respectively. Thus, if a small round hole of diameter d in a large tank ($d/D \approx 0$), the jet diameter would be $(0.611)^{1/2} = 0.782$ times the hole diameter, since $\theta = 90°$.

40.8 DIMENSIONLESS NUMBERS AND DYNAMIC SIMILARITY

Dimensionless numbers are commonly used to plot experimental data to make the results more universal. Some are also used in designing experiments to ensure dynamic similarity between the flow of interest and the flow being studied in the laboratory.

40.8.1 Dimensionless Numbers

Dimensionless numbers or groups may be obtained from force ratios, by a dimensional analysis using the Buckingham Pi theorem, for example, or by writing the differential equations of motion and energy in dimensionless form. Dynamic similarity between two geometrically similar systems exists when the appropriate dimensionless groups are the same for the two systems. This is the basis on which model studies are made, and results measured for one flow may be applied to similar flows.

The dimensions of some parameters used in fluid mechanics are listed in Table 40.5. The mass–length–time (MLT) and the force–length–time (FLT) systems are related by $F = Ma = ML/T^2$ and $M = FT^2/L$.

Force ratios are expressed as

$$\frac{\text{inertia force}}{\text{viscous force}} = \frac{\rho L^2 V^2}{\mu VL} = \frac{\rho LV}{\mu}, \quad \text{the Reynolds number Re}$$

$$\frac{\text{inertia force}}{\text{gravity force}} = \frac{\rho L^2 V^2}{\rho L^3 g} = \frac{V^2}{Lg} \quad \text{or} \quad \frac{V}{\sqrt{Lg}}, \quad \text{the Froude number Fr}$$

$$\frac{\text{pressure force}}{\text{inertia force}} = \frac{\Delta p L^2}{\rho L^2 V^2} = \frac{\Delta p}{\rho V^2} \quad \text{or} \quad \frac{\Delta p}{\rho V^2/2}, \quad \text{the pressure coefficient } C_p$$

$$\frac{\text{inertia force}}{\text{surface tension force}} = \frac{\rho L^2 V^2}{\sigma L} = \frac{V^2}{\sigma/\rho L} \quad \text{or} \quad \frac{V}{\sqrt{\sigma/\rho L}}, \quad \text{the Weber number We}$$

$$\frac{\text{inertia force}}{\text{compressibility force}} = \frac{\rho L^2 V^2}{KL^2} = \frac{V^2}{K/\rho} \quad \text{or} \quad \frac{V}{\sqrt{K/\rho}}, \quad \text{the Mach number M}$$

If a system includes n quantities with m dimensions, there will be at least $n - m$ independent dimensionless groups, each containing m repeating variables. Repeating variables (1) must include all the m dimensions, (2) should include a geometrical characteristic, a fluid property, and a flow characteristic and (3) should not include the dependent variable.

Thus, if the pressure gradient $\Delta p/L$ for flow in a pipe is judged to depend on the pipe diameter D and roughness k, the average flow velocity V, and the fluid density ρ, the fluid viscosity μ, and compressibility K (for gas flow), then $\Delta p/L = f(D, k, V, \rho, \mu, K)$ or in dimensions, $F/L^3 = f(L, L, L/T, FT^2/L^4, FT/L^2, F/L^2)$, where $n = 7$ and $m = 3$. Then there are $n - m = 4$ independent groups to be sought. If D, ρ, and V are the repeating variables, the results are

$$\frac{\Delta p}{\rho V^2/2} = f\left(\frac{DV\rho}{\mu}, \frac{k}{D}, \frac{V}{\sqrt{K/\rho}}\right)$$

or that the friction factor will depend on the Reynolds number of the flow, the relative roughness, and the Mach number. The actual relationship between them is determined experimentally. Results may be determined analytically for laminar flow. The seven original variables are thus expressed as four dimensionless variables, and the Moody diagram of Fig. 40.32 shows the result of analysis and experiment. Experiments show that the pressure gradient does depend on the Mach number, but the friction factor does not.

The Navier–Stokes equations are made dimensionless by dividing each length by a characteristic length L and each velocity by a characteristic velocity U. For a body force X due to gravity, $X = g_x = g(\partial z/\partial x)$. Then $x' = x/L$, etc., $t' = t(L/U)$, $u' = u/U$, etc., and $p' = p/\rho U^2$. Then the Navier–Stokes equation (x component) is

$$\begin{aligned} u' \frac{\partial u'}{\partial x'} &+ v' \frac{\partial u'}{\partial y'} + w' \frac{\partial u'}{\partial z'} + \frac{\partial u'}{\partial t'} \\ &= \frac{gL}{U^2} - \frac{\partial p'}{\partial x'} + \frac{\mu}{\rho UL}\left(\frac{\partial^2 u'}{\partial x'^2} + \frac{\partial^2 u'}{\partial y'^2} + \frac{\partial^2 u'}{\partial z'^2}\right) \\ &= \frac{1}{\text{Fr}^2} - \frac{\partial p'}{\partial x'} + \frac{1}{\text{Re}}\left(\frac{\partial^2 u'}{\partial x'^2} + \frac{\partial^2 u'}{\partial y'^2} + \frac{\partial^2 u'}{\partial z'^2}\right) \end{aligned}$$

Table 40.5 Dimensions of Fluid and Flow Parameters

	FLT	*MLT*
Geometrical characteristics		
Length (diameter, height, breadth, chord, span, etc.)	L	L
Angle	None	None
Area	L^2	L^2
Volume	L^3	L^3
Fluid properties[a]		
Mass	FT^2/L	M
Density (ρ)	FT^2/L^4	M/L^3
Specific weight (γ)	F/L^3	M/L^2T^2
Kinematic viscosity (v)	L^2/T	L^2/T
Dynamic viscosity (μ)	FT/L^2	M/LT
Elastic modulus (K)	F/L^2	M/LT^2
Surface tension (σ)	F/L	M/T^2
Flow characteristics		
Velocity (V)	L/T	L/T
Angular velocity (ω)	$1/T$	$1/T$
Acceleration (a)	L/T^2	L/T^2
Pressure (Δp)	F/L^2	M/LT^2
Force (drag, lift, shear)	F	ML/T^2
Shear stress (τ)	F/L^2	M/LT^2
Pressure gradient ($\Delta p/L$)	F/L^3	M/L^2T^2
Flow rate (Q)	L^3/T	L^3/T
Mass flow rate ($\dot{m}$)	FT/L	M/T
Work or energy	FL	ML^2/T^2
Work or energy per unit weight	L	L
Torque and moment	FL	ML^2/T^2
Work or energy per unit mass	L^2/T^2	L^2/T^2

[a]Density, viscosity, elastic modulus, and surface tension depend upon temperature, and therefore temperature will not be considered a property in the sense used here.

Thus for incompressible flow, similarity of flow in similar situations exists when the Reynolds and the Froude numbers are the same.

For compressible flow, normalizing the differential energy equation in terms of temperatures, pressure, and velocities gives the Reynolds, Mach, and Prandtl numbers as the governing parameters.

40.8.2 Dynamic Similitude

Flow systems are considered to be dynamically similar if the appropriate dimensionless numbers are the same. Model tests of aircraft, missiles, rivers, harbors, breakwaters, pumps, turbines, and so forth are made on this basis. Many practical problems exist, however, and it is not always possible to achieve complete dynamic similarity. When viscous forces govern the flow, the Reynolds number should be the same for model and prototype, the length in the Reynolds number being some characteristic length. When gravity forces govern the flow, the Froude number should be the same. When surface tension forces are significant, the Weber number is used. For compressible gas flow, the Mach number is used; different gases may be used for the model and prototype. The pressure coefficient $C_p = \Delta p/(\rho V^2/2)$, the drag coefficient $C_D = \text{drag}/(\rho V^2/2)A$, and the lift coefficient $C_L = \text{lift}/(\rho V^2/2)A$ will be the same for model and prototype when the appropriate Reynolds, Froude, or Mach number is the same. A cavitation number is used in cavitation studies, $\sigma_v = (p - p_v)/(\rho V^2/2)$ if vapor pressure p_v is the reference pressure or $\sigma_c = (p - p_c)/(\rho V^2/2)$ if a cavity pressure is the reference pressure.

Modeling ratios for conducting tests are listed in Table 40.6. Distorted models are often used for rivers in which the vertical scale ratio might be 1/40 and the horizontal scale ratio 1/100, for example, to avoid surface tension effects and laminar flow in models too shallow.

Incomplete similarity often exists in Froude–Reynolds models since both contain a length parameter. Ship models are tested with the Froude number parameter, and viscous effects are calculated for both model and prototype.

The specific speed of pumps and turbines results from combining groups in a dimensional analysis of rotary systems. That for pumps is $N_{s\,(\text{pump})} = N\sqrt{Q}/e^{3/4}$ and for turbines it is $N_{s\,(\text{turbines})} = N\sqrt{\text{power}}/\rho^{1/2}e^{5/4}$, where N is the rotational speed in rad/sec, Q is the volumetric flow rate in m^3/

Table 40.6 Modeling Ratios[a]

Ratio	Reynolds Number	Froude Number, Undistorted Model[b]	Froude Number, Distorted Model[b]	Mach Number, Same Gas[d]	Mach Number, Different Gas[d]
Velocity					
$\frac{V_m}{V_p}$	$\frac{L_p}{L_m}\frac{\rho_p}{\rho_m}\frac{\mu_m}{\mu_p}$	$\left(\frac{L_m}{L_p}\right)^{1/2}$	$\left(\frac{L_m}{L_p}\right)_V^{1/2}$	$\left(\frac{\theta_m}{\theta_p}\right)^{1/2}$	$\left(\frac{k_m R_m \theta_m}{k_p R_p \theta_p}\right)^{1/2}$
Angular velocity					
$\frac{\omega_m}{\omega_p}$	$\left(\frac{L_p}{L_m}\right)^2\frac{\rho_p}{\rho_m}\frac{\mu_m}{\mu_p}$	$\left(\frac{L_p}{L_m}\right)^{1/2}$	—[c]	$\left(\frac{\theta_m}{\theta_p}\right)^{1/2}\frac{L_p}{L_m}$	$\left(\frac{k_m R_m \theta_m}{k_p R_p \theta_p}\right)^{1/2}\frac{L_p}{L_m}$
Volumetric flow rate					
$\frac{Q_m}{Q_p}$	$\frac{L_m}{L_p}\frac{\rho_p}{\rho_m}\frac{\mu_m}{\mu_p}$	$\left(\frac{L_m}{L_p}\right)^{5/2}$	$\left(\frac{L_m}{L_p}\right)_V^{3/2}\left(\frac{L_m}{L_p}\right)_H$	—[c]	—[c]
Time					
$\frac{t_m}{t_p}$	$\left(\frac{L_m}{L_p}\right)^2\frac{\rho_m}{\rho_p}\frac{\mu_p}{\mu_m}$	$\left(\frac{L_m}{L_p}\right)^{1/2}\left(\frac{g_p}{g_m}\right)^{1/2}$	$\left(\frac{L_m}{L_p}\right)_H\left(\frac{L_p}{L_m}\right)_V^{1/2}\left(\frac{g_p}{g_m}\right)^{1/2}$	$\left(\frac{\theta_p}{\theta_m}\right)^{1/2}\frac{L_m}{L_p}$	$\left(\frac{k_p R_p \theta_p}{k_m R_m \theta_m}\right)^{1/2}\frac{L_m}{L_p}$
Force					
$\frac{F_m}{F_p}$	$\left(\frac{\mu_m}{\mu_p}\right)^2\frac{\rho_p}{\rho_m}$	$\left(\frac{L_m}{L_p}\right)^3\frac{\rho_m}{\rho_p}$	$\frac{\rho_m}{\rho_p}\left(\frac{L_m}{L_p}\right)_H\left(\frac{L_m}{L_p}\right)_V^2$	$\frac{\rho_m}{\rho_p}\frac{\theta_m}{\theta_p}\left(\frac{L_m}{L_p}\right)^2$	$\frac{K_m}{K_p}\left(\frac{L_m}{L_p}\right)^2$

[a]Subscript m indicates model, subscript p indicates prototype.

[b]For the same value of gravitational acceleration for model and prototype.

[c]Of little importance.

[d]Here θ refers to temperature.

sec, and e is the energy in J/kg. North American practice uses N in rpm, Q in gal/min, e as energy per unit weight (head in ft), power as brake horsepower rather than watts, and omits the density term in the specific speed for turbines. The numerical value of specific speed indicates the type of pump or turbine for a given installation. These are shown for pumps in North America in Fig. 40.20. Typical values for North American turbines are about 5 for impulse turbines, about 20–100 for Francis turbines, and 100–200 for propeller turbines. Slight corrections in performance for higher efficiency of large pumps and turbines are made when testing small laboratory units.

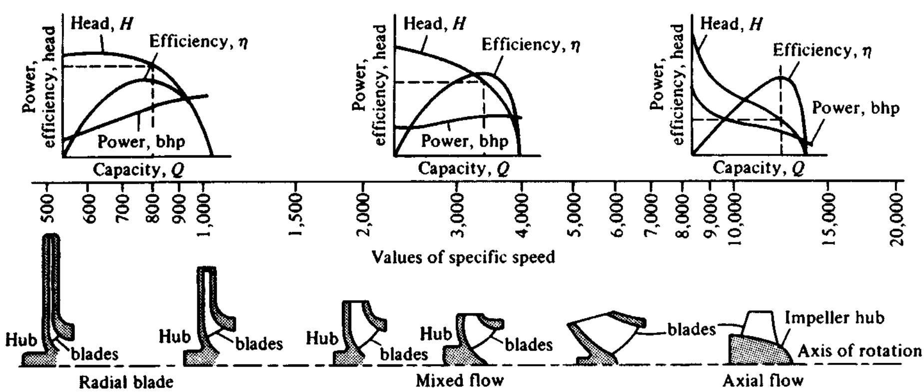

Fig. 40.20 Pump characteristics and specific speed for pump impellers. (Courtesy Worthington Corporation)

40.9 VISCOUS FLOW AND INCOMPRESSIBLE BOUNDARY LAYERS

In viscous flows, adjacent layers of fluid transmit both normal forces and tangential shear forces, as a result of relative motion between the layers. There is no relative motion, however, between the fluid and a solid boundary along which it flows. The fluid velocity varies from zero at the boundary to a maximum or free stream value some distance away from it. This region of retarded flow is called the boundary layer.

40.9.1 Laminar and Turbulent Flow

Viscous fluids flow in a laminar or in a turbulent state. There are, however, transition regimes between them where the flow is intermittently laminar and turbulent. Laminar flow is smooth, quiet flow without lateral motions. Turbulent flow has lateral motions as a result of eddies superimposed on the main flow, which results in random or irregular fluctuations of velocity, pressure, and, possibly, temperature. Smoke rising from a cigarette held at rest in still air has a straight threadlike appearance for a few centimeters; this indicates a laminar flow. Above that the smoke is wavy and finally irregular lateral motions indicate a turbulent flow. Low velocities and high viscous forces are associated with laminar flow and low Reynolds numbers. High speeds and low viscous forces are associated with turbulent flow and high Reynolds numbers. Turbulence is a characteristic of flows, not of fluids. Typical fluctuations of velocity in a turbulent flow are shown in Fig. 40.21.

The axes of eddies in turbulent flow are generally distributed in all directions. In *isotropic* turbulence they are distributed equally. In flows of low turbulence, the fluctuations are small; in highly turbulent flows, they are large. The turbulence level may be defined as (as a percentage)

$$T = \frac{\sqrt{(\overline{u'^2} + \overline{v'^2} + \overline{w'^2})/3}}{\bar{u}} \times 100$$

where u', v', and w' are instantaneous fluctuations from mean values and $\bar{u}$ is the average velocity in the main flow direction (x, in this instance).

Shear stresses in turbulent flows are much greater than in laminar flows for the same velocity gradient and fluid.

40.9.2 Boundary Layers

The growth of a boundary layer along a flat plate in a uniform external flow is shown in Fig. 40.22. The region of retarded flow, δ, thickens in the direction of flow, and thus the velocity changes from zero at the plate surface to the free stream value u_s in an increasingly larger distance δ normal to the plate. Thus, the velocity gradient at the boundary, and hence the shear stress as well, decreases as the flow progresses downstream, as shown. As the laminar boundary thickens, instabilities set in and the boundary layer becomes turbulent. The transition from the laminar boundary layer to a turbulent boundary layer does not occur at a well-defined location; the flow is intermittently laminar and turbulent with a larger portion of the flow being turbulent as the flow passes downstream. Finally, the flow is completely turbulent, and the boundary layer is much thicker and the boundary shear greater in the turbulent region than if the flow were to continue laminar. A viscous sublayer exists within the turbulent boundary layer along the boundary surface. The shape of the velocity profile also changes when the boundary layer becomes turbulent, as shown in Fig. 40.22. Boundary surface roughness, high turbulence level in the outer flow, or a decelerating free stream causes transition to occur nearer the leading edge of the plate. A surface is considered rough if the roughness elements have an effect outside the viscous sublayer, and smooth if they do not. Whether a surface is rough or smooth depends not only on the surface itself but also on the character of the flow passing it.

A boundary layer will separate from a continuous boundary if the fluid within it is caused to slow down such that the velocity gradient du/dy becomes zero at the boundary. An adverse pressure gradient will cause this.

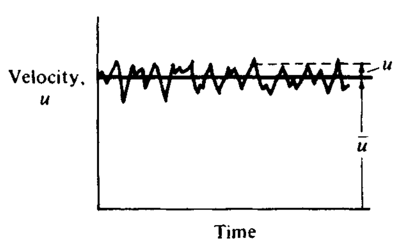

Fig. 40.21 Velocity at a point in steady turbulent flow.

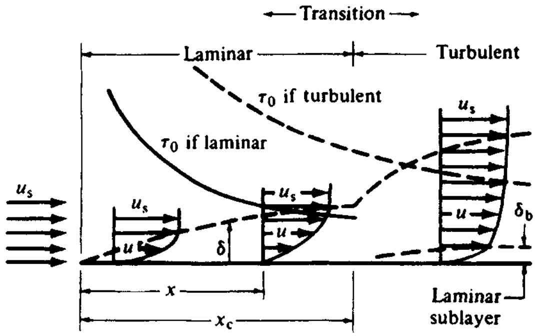

Fig. 40.22 Boundary layer development along a flat plate.

One parameter of interest is the boundary layer thickness δ, the distance from the boundary in which the flow is retarded, or the distance to the point where the velocity is 99% of the free stream velocity (Fig. 40.23). The displacement thickness is the distance the boundary is displaced such that the boundary layer flow is the same as one-dimensional flow past the displaced boundary. It is given by (see Fig. 40.23)

$$\delta_1 = \frac{1}{u_s}\int_0^\delta (u_s - u)\,dy = \int_0^\delta \left(1 - \frac{u}{u_s}\right) dy$$

A momentum thickness is the distance from the boundary such that the momentum flux of the free stream within this distance is the deficit of momentum of the boundary layer flow. It is given by (see Fig. 40.23)

$$\delta_2 = \int_0^\delta \left(1 - \frac{u}{u_s}\right)\frac{u}{u_s}\,dy$$

Also of interest is the viscous shear drag $D = C_f(\rho u_s^2/2)A$, where C_f is the average skin friction drag coefficient and A is the area sheared.

These parameters are listed in Table 40.7 as functions of the Reynolds number $\mathrm{Re}_x = u_s\rho x/\mu$, where x is based on the distance from the leading edge. For Reynolds numbers between 1.8×10^5 and 4.5×10^7, $C_f = 0.045/\mathrm{Re}_x^{1/6}$, and for Re_x between 2.9×10^7 and 5×10^8, $C_f = 0.0305/\mathrm{Re}_x^{1/7}$. These results for turbulent boundary layers are obtained from pipe flow friction measurements for smooth pipes, by assuming the pipe radius equivalent to the boundary layer thickness, the centerline pipe velocity equivalent to the free stream boundary layer flow, and appropriate velocity profiles. Results agree with measurements.

When a turbulent boundary layer is preceded by a laminar boundary layer, the drag coefficient is given by the Prandtl–Schlichting equation:

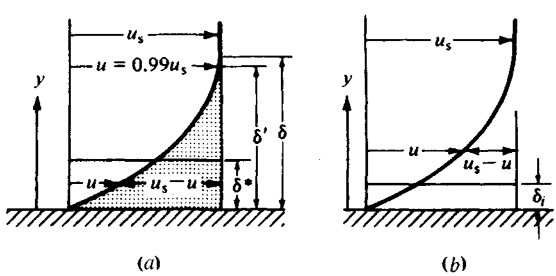

Fig. 40.23 Definition of boundary layer thickness: (a) displacement thickness; (b) momentum thickness.

Table 40.7 Boundary Layer Parameters

Parameter	Laminar Boundary Layer	Turbulent Boundary Layer
$\frac{\delta}{x}$	$\frac{4.91}{\mathrm{Re}_x^{1/2}}$	$\frac{0.382}{\mathrm{Re}_x^{1/5}}$
$\frac{\delta_1}{x}$	$\frac{1.73}{\mathrm{Re}_x^{1/2}}$	$\frac{0.048}{\mathrm{Re}_x^{1/5}}$
$\frac{\delta_2}{x}$	$\frac{0.664}{\mathrm{Re}_x^{1/2}}$	$\frac{0.037}{\mathrm{Re}_x^{1/5}}$
C_f	$\frac{1.328}{\mathrm{Re}_x^{1/2}}$	$\frac{0.074}{\mathrm{Re}_x^{1/5}}$
Re_x range	Generally not over 10^6	Less than 10^7

$$C_f = \frac{0.455}{(\log_{10} \mathrm{Re}_x)^{2.58}} - \frac{A}{\mathrm{Re}_x}$$

where A depends on the Reynolds number Re_c at which transition occurs. Values of A for various values of $\mathrm{Re}_c = u_s x_c / v$ are

Re_c	3×10^5	5×10^5	9×10^5	1.5×10^6
A	1035	1700	3000	4880

Some results are shown in Fig. 40.24 for transition at these Reynolds numbers for completely laminar boundary layers, for completely turbulent boundary layers, and for a typical ship hull. (The other curves are applicable for smooth model ship hulls.) Drag coefficients for flat plates may be used for other shapes that approximate flat plates.

The thickness of the viscous sublayer δ_b in terms of the boundary layer thickness is approximately

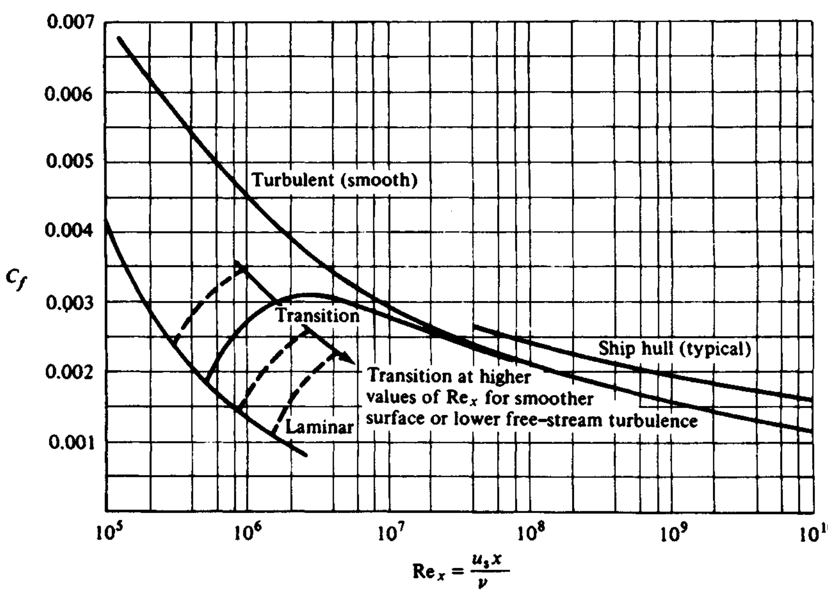

Fig. 40.24 Drag coefficients for smooth plane surfaces parallel to flow.

$$\frac{\delta_b}{\delta} = \frac{80}{(\mathrm{Re}_x)^{7/10}}$$

At $\mathrm{Re}_x = 10^6$, $\delta_b/\delta = 0.0050$ and when $\mathrm{Re}_x = 10^7$, $\delta_b/\delta = 0.001$, and thus the viscous sublayer is very thin.

Experiments show that the boundary layer thickness and local drag coefficient for a turbulent boundary layer preceded by a laminar boundary layer at a given location are the same as though the boundary layer were turbulent from the beginning of the plate or surface along which the boundary layer grows.

40.10 GAS DYNAMICS

In gas flows where density variations are appreciable, large variations in velocity and temperature may also occur and then thermodynamic effects are important.

40.10.1 Adiabatic and Isentropic Flow

In adiabatic flow of a gas with no external work and with changes in elevation negligible, the steady-flow energy equation is

$$\frac{V_1^2}{2} + h_1 = \frac{V_2^2}{2} + h_2 = h_0 = \text{constant}$$

for flow from point 1 to point 2, where V is velocity and h is enthalpy. Subscript 0 refers to a stagnation condition where the velocity is zero.

The speed of sound is $c = \sqrt{(\partial p/\partial s)_{\text{isentropic}}}\ \sqrt{K/\rho} = \sqrt{kp/\rho} = \sqrt{kRT}$. For air, $c = 20.04\sqrt{T}$ m/sec, where T is in degrees kelvin. A local Mach number is then $M = V/c = V/\sqrt{kRT}$.

A gas at rest may be accelerated adiabatically to any speed, including sonic ($M = 1$) and theoretically to its maximum speed when the temperature reduces to absolute zero. Then,

$$c_p T_0 = c_p T + \frac{V^2}{2} = c_p T^* + \frac{V^{*2}}{2} = \frac{V_{\max}^2}{2}$$

where the asterisk (*) refers to a sonic state where the Mach number is unity.

The stagnation temperature T_0 is $T_0 = T + V^2/2c_p$, or in terms of the Mach number $[c_p = Rk/(k - 1)]$

$$\frac{T_0}{T} = 1 + \frac{k-1}{2} M^2 = 1 + 0.2M^2 \text{ for air}$$

The stagnation temperature is reached adiabatically from any velocity V where the Mach number is M and the temperature T. The temperature T^* in terms of the stagnation temperature T_0 is $T^*/T_0 = 2/(k + 1) = 5/6$ for air.

The stagnation pressure is reached reversibly and is thus the isentropic stagnation pressure. It is also called the reservoir pressure, since for any flow a reservoir (stagnation) pressure may be imagined from which the flow proceeds isentropically to a pressure p at a Mach number M. The stagnation pressure p_0 is a constant in isentropic flow; if nonisentropic, but adiabatic, p_0 decreases:

$$\frac{p_0}{p} = \left(\frac{T_0}{T}\right)^{k/(k-1)} = \left(1 + \frac{k-1}{2} M^2\right)^{k/(k-1)} = (1 + 0.2M^2)^{3.5} \text{ for air}$$

Expansion of this expression gives

$$p_0 = p + \frac{\rho V^2}{2}\left[1 + \frac{1}{4}M^2 + \frac{2-k}{24}M^4 + \frac{(2-k)(3-2k)}{192}M^6 + \cdots\right]$$

where the term in brackets is the compressibility factor. It ranges from 1 at very low Mach numbers to a maximum of 1.27 at $M = 1$, and shows the effect of increasing gas density as it is brought to a stagnation condition at increasingly higher initial Mach numbers. The equations are valid to or from a stagnation state for subsonic flow, and from a stagnation state for supersonic flow at M^2 less than $2/(k - 1)$, or M less than $\sqrt{5}$ for air.

40.10.2 Duct Flow

Adiabatic flow in short ducts may be considered reversible, and thus the relation between velocity and area changes is $dA/dV = (A/V)(M^2 - 1)$. For subsonic flow, dA/dV is negative and velocity changes relate to area changes in the same way as for incompressible flow. At supersonic speed, dA/dV is positive and an expanding area is accompanied by an increasing velocity; a contracting area is accompanied by a decreasing velocity, the opposite of incompressible flow behavior. Sonic flow in a duct (at $M = 1$) can exist only when the duct area is constant ($dA/dV = 0$), in the throat of a nozzle or in a pipe. It can also be shown that velocity and Mach numbers always increase or decrease together, that temperature and Mach numbers change in opposite directions, and that pressure and Mach numbers also change in opposite directions.

Isentropic gas flow tables give pressure ratios p/p_0, temperature ratios T/T_0, density ratios ρ/ρ_0, area ratios A/A^*, and velocity ratios V/V^* as functions of the upstream Mach number M_x and the specific heat ratio k for gases.

The mass flow rate through a converging nozzle from a reservoir with the gas at a pressure p_0 and temperature T_0 is calculated in terms of the pressure at the nozzle exit from the equation $\dot{m} = (VA\rho)_{\text{exit}}$, where $\rho_e = p_e/RT_e$ and the exit temperature is $T_e = T_0(p_e/p_0)^{(k-1)/k}$ and the exit velocity is

$$V_e = \sqrt{2c_pT_0\left[1 - \left(\frac{p_e}{p_0}\right)^{(k-1)/k}\right]}$$

The mass flow rate is maximum when the exit velocity is sonic. This requires the exit pressure to be critical, and the receiver pressure to be critical or below. Supersonic flow in the nozzle is impossible. If the receiver pressure is below critical, flow is not affected in the nozzle, and the exit flow remains sonic. For air at this condition, the maximum flow rate is $\dot{m} = 0.0404A_1p_0/\sqrt{T_0}$ kg/sec.

Flow through a converging–diverging nozzle (Fig. 40.25) is subsonic throughout if the throat pressure is above critical (dashed lines in Fig. 40.25). When the receiver pressure is at A, the exit pressure is also, and sonic flow exists at the throat, but is subsonic elsewhere. Only at B is there sonic flow in the throat with isentropic expansion in the diverging part of the nozzle. The flow rate is the same whether the exit pressure is at A or B. Receiver pressures below B do not affect the flow in the nozzle. Below A (at C, for example) a shock forms as shown and then the flow is isentropic to the shock, and beyond it, but not through it. When the throat flow is sonic, the mass flow rate is given by the same equation as for a converging nozzle with sonic exit flow. The pressures at A and B in terms of the reservoir pressure p_0 are given in isentropic flow tables as a function of the ratio of exit area to throat area, A_c/A^*.

40.10.3 Normal Shocks

The plane of a normal shock is at right angles to the flow streamlines. These shocks may occur in the diverging part of a nozzle, the diffuser of a supersonic wind tunnel, in pipes and forward of blunt-nosed bodies. In all instances the flow is supersonic upstream and subsonic downstream of the shock. Flow through a shock is not isentropic, although nearly so for very weak shocks. The abrupt changes in gas density across a shock allow for optical detection. The interferometer responds to density changes, the Schlieren method to density gradients, and the spark shadowgraph to the rate of change of density gradient. Density ratios across normal shocks in air are 2 at $M = 1.58$, 3 at $M = 2.24$, and 4 at $M = 3.16$ to a maximum value of 6.

Changes in fluid and flow parameters across normal shocks are obtained from the continuity, energy, and momentum equations for adiabatic flow. They are expressed in terms of upstream Mach numbers with upstream conditions designated with subscript x and downstream with subscript y. Mach numbers M_x and M_y are related by

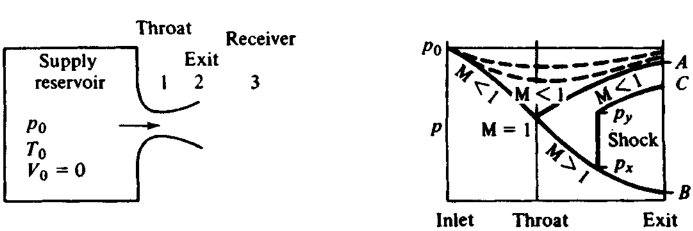

Fig. 40.25 Gas flow through converging–diverging nozzle.

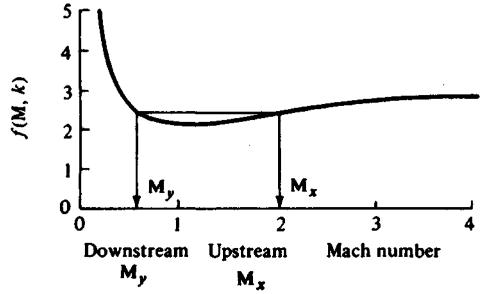

Fig. 40.26 Mach numbers across a normal shock, $k = 1.4$.

$$\frac{1 + kM_x^2}{M_x\left(1 + \frac{k-1}{2}M_x^2\right)^{1/2}} = \frac{1 + kM_y^2}{M_y\left(1 + \frac{k-1}{2}M_y^2\right)^{1/2}} = f(M,k)$$

which is plotted in Fig. 40.26. The requirement for an entropy increase through the shock indicates M_x to be greater than M_y. Thus, the higher the upstream Mach number, the lower the downstream Mach number, and vice versa. For normal shocks, values of downstream Mach number M_y; temperature ratios T_y/T_x; pressure ratios p_y/p_x, p_{0y}/p_x, and p_{0y}/p_{0x}; and density ratios ρ_y/ρ_x depend only on the upstream Mach number M_x and the specific heat ratio k of the gas. These values are tabulated in books on gas dynamics and in books of gas tables.

The density ratio across the shock is given by the Rankine–Hugoniot equation

$$\frac{\rho_y}{\rho_x} = \left[\left(\frac{k+1}{k-1}\right)\frac{p_y}{p_x} + 1\right] \Big/ \left[\frac{p_y}{p_x} + \left(\frac{k+1}{k-1}\right)\right]$$

and is plotted in Fig. 40.27, which shows that weak shocks are nearly isentropic, and that the density ratio approaches a limit of 6 for gases with $k = 1.4$.

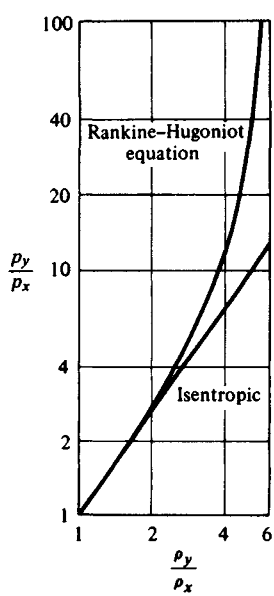

Fig. 40.27 Rankine–Hugoniot curve, $k = 1.4$.

Gas tables show that at an upstream Mach number of 2 for air, $M_y = 0.577$, the pressure ratio is $p_y/p_x = 4.50$, the density ratio is $\rho_y/\rho_x = 2.66$, the temperature ratio is $T_y/T_x = 1.68$, and the stagnation pressure ratio is $p_{0y}/p_{0x} = 0.72$, which indicates an entropy increase of $s_y - s_x = -R \ln(p_{0y}/p_{0x}) = 94$ J/kg.

40.10.4 Oblique Shocks

Oblique shocks are inclined from a direction normal to the approaching streamlines. Figure 40.28 shows that the normal velocity components are related by the normal shock relations. From a momentum analysis, the tangential velocity components are unchanged through oblique shocks. The upstream Mach number M_1 is given in terms of the deflection angle θ, the shock angle β, and the specific heat ratio k for the gas as

$$\frac{1}{M_1^2} = \sin^2\beta - \frac{(k+1)}{2}\frac{\sin\beta\sin\theta}{\cos(\beta-\theta)}$$

The geometry is shown in Fig. 40.29, and the variables in this equation are illustrated in Fig. 40.30. For each M_1 there is the possibility of two wave angles β for a given deflection angle θ. The larger wave angle is for strong shocks, with subsonic downstream flow. The smaller wave angle is for weak shocks, generally with supersonic downstream flow at a Mach number less than M_1.

Normal shock tables are used for oblique shocks if M_x is used for $M_1 \sin\beta$. Then $M_y = M_2 \sin(\beta - \theta)$ and other ratios of property values (pressure, temperature, and density) are the same as for normal shocks.

40.11 VISCOUS FLUID FLOW IN DUCTS

The development of flow in the entrance of a pipe with the development of the boundary layer is shown in Fig. 40.31. Wall shear stress is very large at the entrance, and generally decreases in the flow direction to a constant value, as does the pressure gradient dp/dx. The velocity profile also

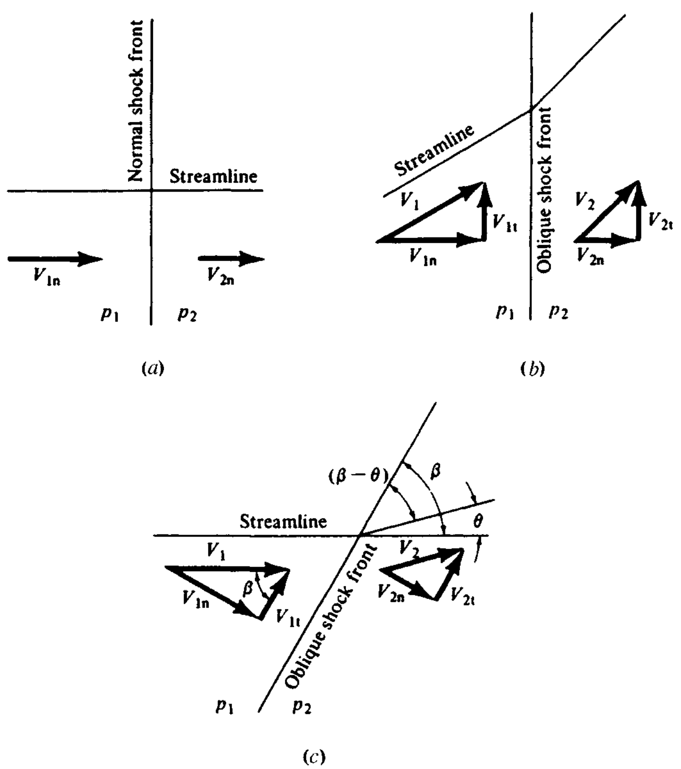

Fig. 40.28 Oblique shock relations from normal shock; (a) normal shock; (b) oblique shock; (c) oblique shock angles.

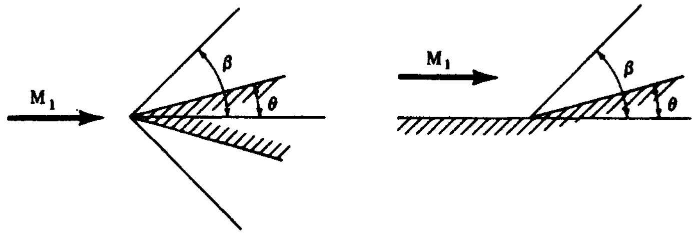

Fig. 40.29 Supersonic flow past a wedge and an inside corner.

changes and becomes adjusted to a fixed shape. When these have reached constant conditions, the flow is called *fully developed* flow.

The momentum equation for a pipe of diameter D gives the pressure gradient as

$$-\frac{dp}{dx} = \frac{4}{D}\tau_0 + \rho V^2 \frac{d\beta}{dx} + \beta\rho V \frac{dV}{dx}$$

which shows that a pressure gradient overcomes wall shear and increases momentum of the fluid either as a result of changing the shape of the velocity profile ($d\beta/dx$) or by changing the mean velocity along the pipe (dV/dx is not zero for gas flows).

For fully developed incompressible flow

$$-\frac{dp}{dx} = \frac{\Delta p}{L} = \frac{4\tau_0}{D}$$

and a pressure drop simply overcomes wall shear.

For developing flow in the entrance, $\beta = 1$ initially and increases to a constant value downstream. Thus, the pressure gradient overcomes wall shear and also increases the flow momentum according to

$$-\frac{dp}{dx} = \frac{4\tau_0}{D} + \rho V^2 \frac{d\beta}{dx}$$

For fully developed flow, $\beta = 4/3$ for laminar flow and $\beta \approx 1.03$ for turbulent flow in round pipes.

For compressible gas flow beyond the entrance, the velocity profile becomes essentially fixed in shape, but the velocity changes because of thermodynamic effects that change the density. Thus, the pressure gradient is

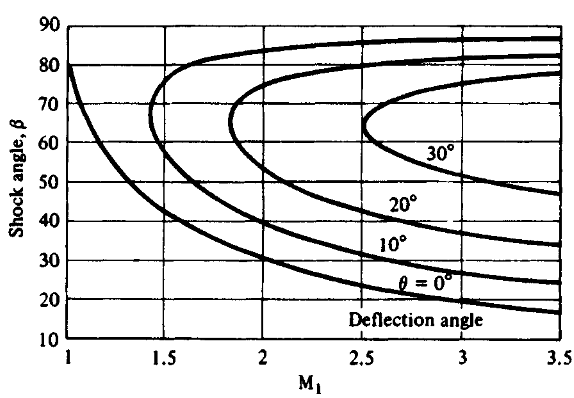

Fig. 40.30 Oblique shock relations, $k = 1.4$.

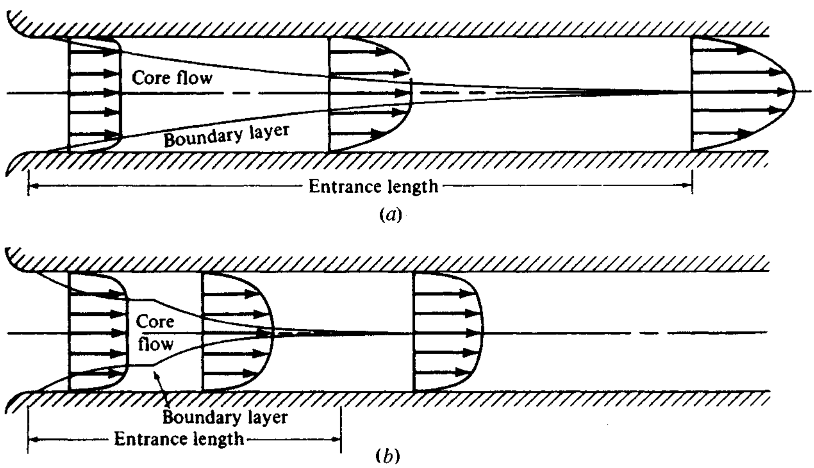

Fig. 40.31 Growth of boundary layers in a pipe: (a) laminar flow; (b) turbulent flow.

$$-\frac{dp}{dx} = \frac{4\tau_0}{D} + \beta\rho V\frac{dV}{dx}$$

Here β is essentially constant but dV/dx may be significant.

40.11.1 Fully Developed Incompressible Flow

The pressure drop is $\Delta p = (fL/D)(\rho V^2/2)$ Pa, where f is the Darcy friction factor. The Fanning friction factor $f' = f/4$ and then $\Delta p = (4f'/D)(\rho V^2/2)$, and the head loss from pipe friction is

$$h_f = \frac{\Delta p}{\gamma} = f\left(\frac{L}{D}\right)\frac{V^2}{2g} = (4f')\left(\frac{L}{D}\right)\frac{V^2}{2g} \quad \text{m}$$

The shear stress varies linearly with radial position, $\tau = (\Delta p/L)(r/2)$, so that the wall shear is $\tau_0 = (\Delta p/L)(D/4)$, which may then be written $\tau_0 = f\rho V^2/8 = f'\rho V^2/2$.

A shear velocity is defined as $v_{\bullet} = \sqrt{\tau_0/\rho} = V\sqrt{f/8} = V\sqrt{f'/2}$ and is used as a normalizing parameter.

For noncircular ducts the diameter D is replaced by the hydraulic or equivalent diameter $D_h = 4A/P$, where A is the flow cross section and P is the wetted perimeter. Thus, an annulus between pipes of diameter D_1 and D_2, D_1 being larger, the hydraulic diameter is $D_2 - D_1$.

40.11.2 Fully Developed Laminar Flow in Ducts

The velocity profile in circular tubes is that of a parabola, and the centerline velocity is

$$u_{max} = \frac{\Delta p}{L}\left(\frac{R^2}{4\mu}\right)$$

and the velocity profile is

$$\frac{u}{u_{max}} = 1 - \left(\frac{r}{R}\right)^2$$

where r is the radial location in a pipe of radius R. The average velocity is one-half the maximum velocity, $V = u_{max}/2$.

The pressure gradient is

$$\frac{\Delta p}{L} = \frac{128\mu Q}{\pi D^4}$$

which indicates a linear increase with increasing velocity or flow rate. The friction factor for circular ducts is $f = 64/\mathrm{Re}_D$ or $f' = 16/\mathrm{Re}_D$ and applies to both smooth as well as rough pipes, for Reynolds numbers up to about 2000.

For *noncircular* ducts the value of the friction factor is $f = C/\mathrm{Re}$ and depends on the duct geometry. Values of $f\ \mathrm{Re} = C$ are listed in Table 40.8.

40.11.3 Fully Developed Turbulent Flow in Ducts

Knowledge of turbulent flow in ducts is based on physical models and experiments. Physical models describe lateral transport of fluid as a result of mixing due to eddies. Prandtl and von Kármán both derived expressions for shear stresses in turbulent flow based on the Reynolds stress ($\tau = -\rho\overline{u'v'}$) and obtained velocity defect equations for pipe flow. Prandtl's equation is

$$\frac{u_{\max} - u}{\sqrt{\tau_0/\rho}} = \frac{u_{\max} - u}{v_*} = 2.5 \ln \frac{R}{y}$$

Table 40.8 Friction Factors for Laminar Flow

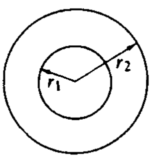

r_1/r_2	f Re
0.0001	71.78
0.001	74.68
0.01	80.11
0.05	86.27
0.10	89.37
0.20	92.35
0.40	94.71
0.60	95.59
0.80	95.92
1.00	96.00

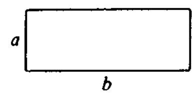

a/b	f Re
0	96.00
1/20	89.91
1/10	84.68
1/8	82.34
1/6	78.81
1/4	72.93
2/5	65.47
1/2	62.19
3/4	57.89
1	56.91

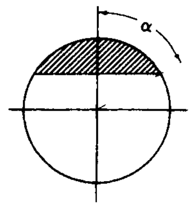

x	f Re
0	62.2
10	62.2
20	62.3
30	62.4
40	62.5
60	62.8
90	63.1
120	63.3
150	63.7
180	64.0

Circular Sector

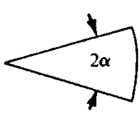

Isosceles Triangle

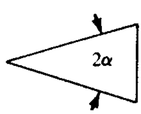

Right Triangle

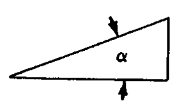

	Circular Sector	Isosceles Triangle	Right Triangle
α	f Re	f Re	f Re
0	48.0	48.0	48.0
10	51.8	51.6	49.9
20	54.5	52.9	51.2
30	56.7	53.3	52.0
40	58.4	52.9	52.4
50	59.7	52.0	52.4
60	60.8	51.1	52.0
70	61.7	49.5	51.2
80	62.5	48.3	49.9
90	63.1	48.0	48.0

where u_{max} is the centerline velocity and u is the velocity a distance y from the pipe wall. von Kármán's equation is

$$\frac{u_{max} - u}{\sqrt{\tau_0/\rho}} = \frac{u_{max} - u}{v_*} = -\frac{1}{\kappa}\left[\ln\left(1 - \sqrt{1 - \frac{y}{R}}\right) + \sqrt{1 - \frac{y}{R}}\right]$$

In both, κ is an experimentally determined constant equal to 0.4 (some experiments show better agreement when $\kappa = 0.36$). Similar expressions apply to external boundary layer flow when the pipe radius R is replaced by the boundary layer thickness δ. Friction factors for smooth pipes have been developed from these results. One is the Blasius equation for $\mathrm{Re}_D = 10^5$ and is $f = 0.316/\mathrm{Re}_D^{1/4}$ obtained by using a power-law velocity profile $u/u_{max} = (y/R)^{1/7}$. The value 7 here increases to 10 at higher Reynolds numbers. The use of a logarithmic form of velocity profile gives the Prandtl law of pipe friction for smooth pipes:

$$\frac{1}{\sqrt{f}} = 2\log(\mathrm{Re}_D\sqrt{f}) - 0.8$$

which agrees well with experimental values. A more explicit formula by Colebrook is $1/\sqrt{f} = 1.8 \log(\mathrm{Re}_D/6.9)$, which is within 1% of the Prandtl equation over the entire range of turbulent Reynolds numbers.

The logarithmic velocity defect profiles apply for *rough* pipes as well as for smooth pipes, since the velocity defect $(u_{max} - u)$ decreases linearly with the shear velocity v_*, keeping the ratio of the two constant.

A relation between the centerline velocity and the average velocity is $u_{max}/V = 1 + 133\sqrt{f}$, which may be used to estimate the average velocity from a single centerline measurement.

The Colebrook–White equation encompasses all turbulent flow regimes, for both smooth and rough pipes:

$$\frac{1}{\sqrt{f}} = 1.74 - 2\log\left(\frac{2k}{D} + \frac{18.7}{\mathrm{Re}_D\sqrt{f}}\right)$$

and this is plotted in Fig. 40.32, where k is the equivalent sand-grain roughness. A simpler equation by Haaland is

$$\frac{1}{\sqrt{f}} = -1.8\log\left[\frac{6.9}{\mathrm{Re}_D} + \left(\frac{k}{3.7D}\right)^{1.11}\right]$$

which is explicit in f and is within 1.5% of the Colebrook–White equation in the range $4000 \leqq \mathrm{Re}_D \leqq 10^8$ and $0 \leqq k/D \leqq 0.05$.

Three types of problems may be solved:

1. *The Pressure Drop or Head Loss.* The Reynolds number and relative roughness are determined and calculations are made directly.
2. *The Flow Rate for Given Fluid and Pressure Drops or Head Loss.* Assume a friction factor, based on a high Re_D for a rough pipe, and determine the velocity from the Darcy equation. Calculate a Re_D, get a better f, and repeat until successive velocities are the same. A second method is to assume a flow rate and calculate the pressure drop or head loss. Repeat until results agree with the given pressure drop or head loss. A plot of Q versus h_L, for example, for a few trials may be used.
3. *A Pipe Size.* Assume a pipe size and calculate the pressure drop or head loss. Compare with given values: Repeat until agreement is reached. A plot of D versus h_L, for example, for a few trials may be used. A second method is to assume a reasonable friction factor and get a first estimate of the diameter from

$$D = \left[\frac{8fLQ^2}{\pi^2 g h_f}\right]^{1/5}$$

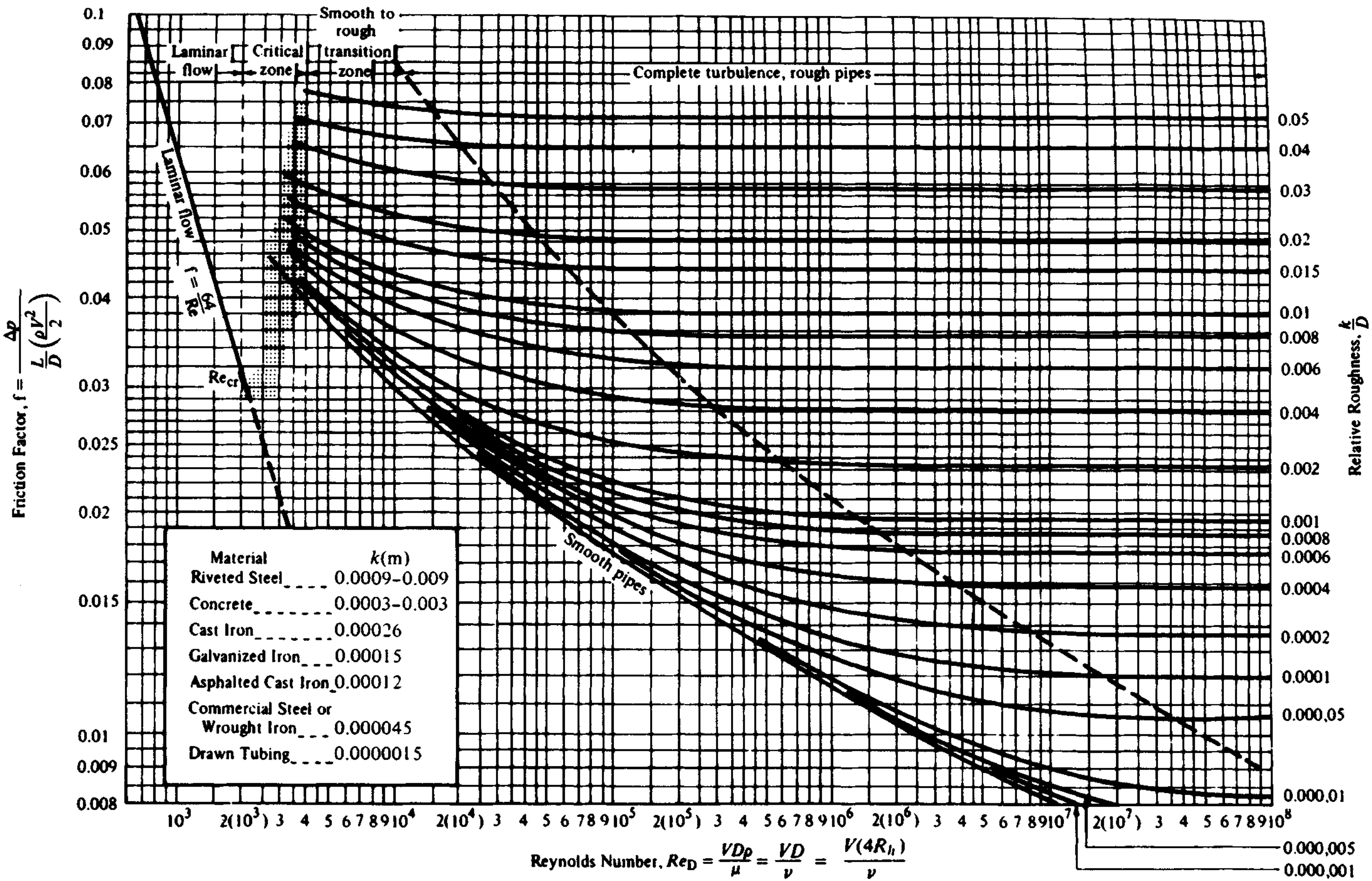

Fig. 40.32 Friction factors for commercial pipe. [From L. F. Moody, "Friction Factors for Pipe Flow," *Trans. ASME,* 66 (1944). Courtesy of The American Society of Mechanical Engineers.]

From the first estimate of D, calculate the Re_D and k/D to get a better value of f. Repeat until successive values of D agree. This is a rapid method.

Results for circular pipes may be applied to noncircular ducts if the hydraulic diameter is used in place of the diameter of a circular pipe. Then the relative roughness is k/D_h and the Reynolds number is $\mathrm{Re} = VD_h/v$. Results are reasonably good for square ducts, rectangular ducts of aspect ratio up to about 8, equilateral ducts, hexagonal ducts, and concentric annular ducts of diameter ratio to about 0.75. In eccentric annular ducts where the pipes touch or nearly touch, and in tall narrow triangular ducts, both laminar and turbulent flow may exist at a section. Analyses mentioned here do not apply to these geometries.

40.11.4 Steady Incompressible Flow in Entrances of Ducts

The increased pressure drop in the entrance region of ducts as compared with that for the same length of fully developed flow is generally included in a correction term called a loss coefficient, k_L. Then,

$$\frac{p_1 - p}{\rho V^2/2} = \frac{fL}{D_h} + k_L$$

where p_1 is the pressure at the duct inlet and p is the pressure a distance L from the inlet. The value of k_L depends on L but becomes a constant in the fully developed region, and this constant value is of greatest interest.

For *laminar* flow the pressure drop in the entrance length L_e is obtained from the Bernoulli equation written along the duct axis where there is no shear in the core flow. This is

$$p_1 - p_e = \frac{\rho u_{\max}^2}{2} - \frac{\rho V^2}{2} = \left[\left(\frac{u_{\max}}{V}\right)^2 - 1\right]\frac{\rho V^2}{2}$$

for any duct for which $u_{\max}/V$ is known. When both friction factor and k_L are known, the entrance length is

$$\frac{L_e}{D_h} = \frac{1}{f}\left[\left(\frac{u_{\max}}{V}\right)^2 - 1 - k_L\right]$$

For a circular duct, experiments and analyses indicate that $k_L \approx 1.30$. Thus, for a circular duct, $L_e/D = (\mathrm{Re}_D/64)(2^2 - 1 - 1.30) = 0.027\mathrm{Re}_D$. The pressure drop for fully developed flow in a length L_e is $\Delta p = 1.70\rho V^2/2$ and thus the pressure drop in the entrance is $3/1.70 = 1.76$ times that in an equal length for fully developed flow. Entrance effects are important for short ducts.

Some values of k_L and $(L_e/D_h)\mathrm{Re}$ for laminar flow in various ducts are listed in Table 40.9.

For turbulent flow, loss coefficients are determined experimentally. Results are shown in Fig. 40.33. Flow separation accounts for the high loss coefficients for the square and reentrant shapes for circular tubes and concentric annuli. For a rounded entrance, a radius of curvature of $D/7$ or more precludes separation. The boundary layer starts laminar then changes to turbulent, and the pressure drop does not significantly exceed the corresponding value for fully developed flow in the same length. (It may even be less with the laminar boundary layer—a trip or slight roughness may force a turbulent boundary layer to exist at the entrance.)

Entrance lengths for circular ducts and concentric annuli are defined as the distance required for the pressure gradient to become within a specified percentage of the fully developed value (5%, for example). On this basis L_e/D_h is about 30 or less.

40.11.5 Local Losses in Contractions, Expansions, and Pipe Fittings; Turbulent Flow

Calculations of local head losses generally are approximate at best unless experimental data for given fittings are provided by the manufacturer.

Losses in *contractions* are given by $h_L = k_L V^2/2g$. Loss coefficients for a sudden contraction are shown in Fig. 40.34. For gradually contracting sections k_L may be as low as 0.03 for D_2/D_1 of 0.5 or less.

Losses in expansions are given by $h_L = k_L(V_1 - V_2)^2/2g$, section 1 being upstream. For a sudden expansion, $k_L = 1$, and for gradually expanding sections with divergence angles of 7° or 8°, k_L may be as low as 0.14 or even 0.06 for diffusers for low-speed wind tunnels or cavitation-testing water tunnels with curved inlets to avoid separation.

Losses in pipe fittings are given in the form $h_L = k_L V^2/2g$ or in terms of an equivalent pipe length by pipe-fitting manufacturers. Typical values for various fittings are given in Table 40.10.

Table 40.9 Entrance Effects, Laminar Flow (See Table 40.8 for Symbols)

r_1/r_2	k_L
0.0001	1.13
0.001	1.07
0.01	0.97
0.05	0.86
0.10	0.81
0.20	0.75
0.40	0.71
0.60	0.69
0.80	0.69
1.00	0.69

a/b	k_L	$L_c D_h Re$
0	0.69	0.0059
1/8	0.88	0.0094
1/5	1.00	0.0123
1/4	1.08	0.0146
1/2	1.38	0.0254
3/4	1.52	0.0311
1	1.55	0.0324

x	k_L
0	1.74
10	1.73
20	1.72
30	1.69
40	1.65
60	1.57
90	1.46
120	1.39
150	1.34
180	1.33

α	Circular Sector k_L	Isosceles Triangle k_L	Right Triangle k_L
0	2.97	2.97	2.97
10	2.06	2.14	2.40
20	1.71	1.85	2.09
30	1.58	1.79	1.94
40	1.53	1.83	1.88
50	1.50	1.95	1.88
60	1.49	2.14	1.94
70	1.48	2.38	2.09
80	1.47	2.72	2.40
90	1.46	2.97	2.97

40.11.6 Flow of Compressible Gases in Pipes with Friction

Subsonic gas flow in pipes involves a decrease in gas density and an increase in gas velocity in the direction of flow. The momentum equation for this flow may be written as

$$\frac{dp}{\rho V^2/2} + f\frac{dx}{D} + 2\frac{dV}{V} = 0$$

For *isothermal* flow the first term is $(2/\rho_1 V_1^2 p_1)p\,dp$, where the subscript 1 refers to an upstream section where all conditions are known. For $L = x_2 - x_1$, integration gives

$$p_1^2 - p_2^2 = \rho_1 V_1^2 p_1 \left(f\frac{L}{D} - 2\ln\frac{p_2}{p_1}\right)$$

or, in terms of the initial Mach number,

$$p_1^2 - p_2^2 = kM_1^2 p_1^2 \left(f\frac{L}{D} - 2\ln\frac{p_2}{p_1}\right)$$

The downstream pressure p_2 at a distance L from section 1 may be obtained by trial by neglecting

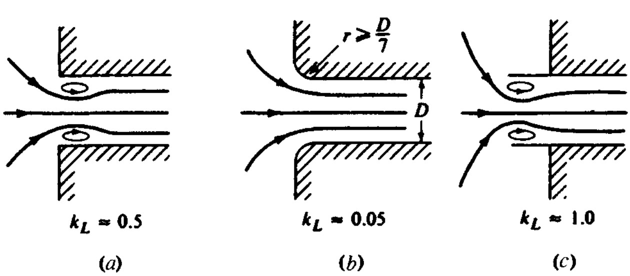

Fig. 40.33 Pipe entrance flows: (*a*) square entrance; (*b*) round entrance; (*c*) reentrant inlet.

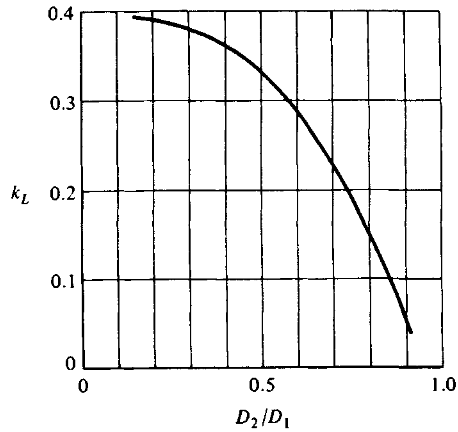

Fig. 40.34 Loss coefficients for abrupt contract in pipes.

the term $2 \ln(p_2/p_1)$ initially to get a p_2, then including it for an improved value. The distance L is a section where the pressure is p_2 is obtained from

$$f\frac{L}{D} = \frac{1}{kM_1^2}\left[1 - \left(\frac{p_2}{p_1}\right)^2\right] - 2\ln\frac{p_1}{p_2}$$

A limiting condition (designated by an asterisk) at a length L^* is obtained from an expression dp/dx to get

Table 40.10 Typical Loss Coefficients for Valves and Fittings

	Nominal Diameter, CM					
Valve or Fitting	2.5	5	10	15	20	25
Globe valve, wide open:						
Screwed	9	7	5.5			
Flanged	12	9	6	6	5.5	5.5
Gate valve, wide open:						
Screwed	0.24	0.18	0.13			
Flanged		0.35	0.16	0.11	0.08	0.06
Foot valve, wide open			0.80 for all sizes			
Swing check valve, wide open						
Screwed	3.0	2.3	2.1			
Flanged			2.0 for all sizes			
Angle valve, wide open:						
Screwed	4.5	2.1	1.0			
Flanged		2.4	2.1	2.1	2.1	2.1
Regular elbow, 90°						
Screwed	1.5	1.0	0.65			
Flanged	0.42	0.37	0.31	0.28	0.26	0.25
Long-radius elbow, 90°						
Screwed	0.75	0.4	0.25			
Flanged		0.3	0.22	0.18	0.15	0.14

Note: The k_L values listed may be expressed in terms of an equivalent pipe length for a given installation and flow by equating $k_L = fL_e/D$ so that $L_e = k_L D/f$.

SOURCE: Reproduced, with permission, from Engineering Data Book: Pipe Friction Manual (Cleveland: Hydraulic Institute, 1979).

$$\frac{dp}{dx} = \frac{pf/2D}{1 - p/\rho V^2} = \frac{(f/D)(\rho V^2/2)}{kM^2 - 1}$$

For a low subsonic flow at an upstream section (as from a compressor discharge) the pressure gradient increases in the flow direction with an infinite value when $M^* = 1/\sqrt{k} = 0.845$ for $k = 1.4$ (air, for example). For M approaching zero, this equation is the Darcy equation for incompressible flow. The limiting pressure is $p^* = p_1 M_1 \sqrt{k}$, and the limiting length is given by

$$\frac{fL^*}{D} = \frac{1}{kM_1^2} - 1 - \ln \frac{1}{kM_1^2}$$

Since the gas at any two locations 1 and 2 in a long pipe has the same limiting condition, the distance L between them is

$$\frac{fL}{D} = \left(\frac{fL^*}{D}\right)_{M_1} - \left(\frac{fL^*}{D}\right)_{M_2}$$

Conditions along a pipe for various initial Mach numbers are shown in Fig. 40.35.

For *adiabatic* flow the limiting Mach number is $M^* = 1$. This is from an expression for dp/dx for adiabatic flow:

$$\frac{dp}{dx} = -\frac{fkp}{2D} M^2 \left[\frac{1 + (k-1)M^2}{1 - M^2}\right] = -\frac{f}{D}\frac{\rho V^2}{2}\left[\frac{1 + (k-1)M^2}{1 - M^2}\right]$$

The limiting pressure is

$$\frac{p^*}{p_1} = M_1 \sqrt{\frac{2[1 + \frac{1}{2}(k-1)M_1^2]}{k+1}}$$

and the limiting length is

$$\frac{\bar{f}L^*}{D} = \frac{1 - M_1^2}{kM_1^2} + \frac{k+1}{2k} \ln \frac{(k+1)M_1^2}{2[1 + \frac{1}{2}(k-1)M_1^2]}$$

Except for subsonic flow at high Mach numbers, isothermal and adiabatic flow do not differ appreciably. Thus, since flow near the limiting condition is not recommended in gas transmission

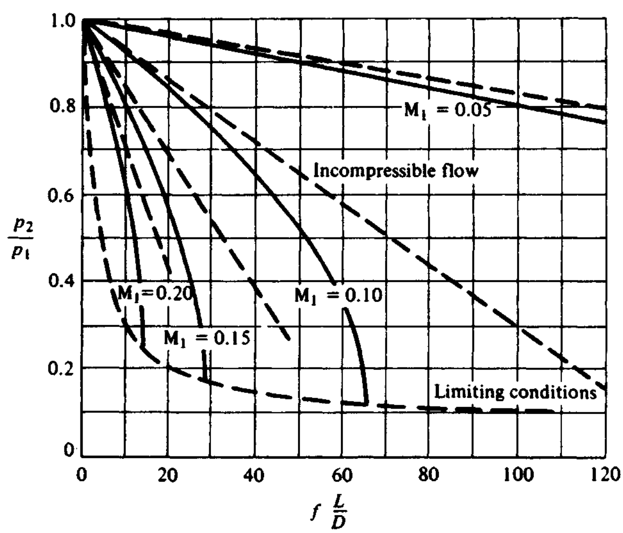

Fig. 40.35 Isothermal gas flow in a pipe for various initial Mach numbers, $k = 1.4$.

pipelines because of the excessive pressure drop, and since purely isothermal or purely adiabatic flow is unlikely, either adiabatic or isothermal flow may be assumed in making engineering calculations. For example, for methane from a compressor at 2000 kPa absolute pressure, 60°C temperature and 15 m/sec velocity ($M_1 = 0.032$) in a 30-cm commercial steel pipe, the limiting pressure is 72 kPa absolute at $L^* = 16.9$ km for isothermal flow, and 59 kPa at $L^* = 17.0$ km for adiabatic flow. A pressure of 500 kPa absolute would exist at 16.0 km for either type of flow.

40.12 DYNAMIC DRAG AND LIFT

Two types of forces act on a body past which a fluid flows: a pressure force normal to any infinitesimal area of the body and a shear force tangential to this area. The components of these two forces integrate over the entire body in a direction parallel to the approach flow is the *drag* force, and in a direction normal to it is the *lift* force. *Induced* drag is associated with a lift force on finite airfoils or blank elements as a result of downwash from tip vortices. Surface waves set up by ships or hydrofoils, and compression waves in gases such as Mach cones are the source of *wave* drag.

40.12.1 Drag

A drag force is $D = C(\rho u_s^2/2)A$, where C is the drag coefficient, $\rho u_s^2/2$ is the dynamic pressure of the free stream, and A is an appropriate area. For pure viscous shear drag C is C_f, the skin friction drag coefficient of Section 40.9.2 and A is the area sheared. In general, C is designated C_D, the drag coefficient for drag other than that from viscous shear only, and A is the chord area for lifting vanes or the projected frontal area for other shapes.

The drag coefficient for incompressible flow with pure pressure drag (a flat plate normal to a flow, for example) or for combined skin friction and pressure drag, which is called *profile* drag, depends on the body shape, the Reynolds number, and, usually, the location of boundary layer transition.

Drag coefficients for spheres and for flow normal to infinite circular cylinders are shown in Fig. 40.36. For spheres at $\mathrm{Re}_D < 0.1$, $C_D = 24/\mathrm{Re}_D$ and for $\mathrm{Re}_D < 100$, $C_D = (24/\mathrm{Re}_D)(1 + 3\,\mathrm{Re}_D/16)^{1/2}$. The boundary layer for both shapes up to and including the flat portion of the curves before the rather abrupt drop in the neighborhood of $\mathrm{Re}_D = 10^5$ is laminar. This is called the *subcritical* region; beyond that is the *supercritical* region. Table 40.11 lists typical drag coefficients for two-dimensional shapes, and Table 40.12 lists them for three-dimensional shapes.

The drag of spheres, circular cylinders, and streamlined shapes is affected by boundary layer separation, which, in turn, depends on surface roughness, the Reynolds number, and free stream turbulence. These factors contribute to uncertainties in the value of the drag coefficient.

40.12.2 Lift

Lift in a nonviscous fluid may be produced by prescribing a circulation around a cylinder or lifting vane. In a viscous fluid this may be produced by spinning a ping-pong ball, a golf ball, or a baseball, for example, Circulation around a lifting vane in a viscous fluid results from the bound vortex or countercirculation that is equal and opposite to the starting vortex, which peels off the trailing edge of the vane. The lift is calculated from $L = C_L(\rho u_s^2/2)A$, where C_L is the lift coefficient, $\rho u_s^2/2$ is the

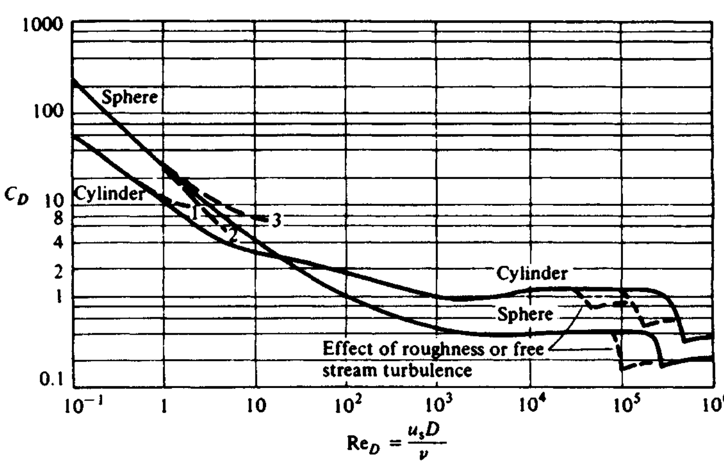

Fig. 40.36 Drag coefficients for infinite circular cylinders and spheres: (1) Lamb's solution for cylinder; (2) Stokes' solution for sphere; (3) Oseen's solution for sphere.

Table 40.11 Drag Coefficients for Two-Dimensional Shapes at Re = 10^5 Based on Frontal Projected Area (Flow is from Left to Right)

Shape		C_D	Shape	C_D	
Plate	|	2.0	Rectangle		
			1:1	1.18	
Open tube	(	1.2	5:1	1.2	
	)	2.3	10:1	1.3	
			20:1	1.5	
Half cylinder	◖	1.16	Elliptical	Below	Above
	◗	1.7	Cylinder	Re_c	Re_c
			2:1	0.6	0.20
Square cylinder	□	2.05	4:1	0.36	0.10
	◇	1.55	8:1	0.26	0.10
Equilateral triangle	▷	2.0			
	◁	1.6			

dynamic pressure of the free stream, and A is the chord area of the lifting vane. Typical values of C_L as well as C_D are shown in Fig. 40.37. The induced drag and the profile drag are shown. The profile drag is the difference between the dashed and solid curves. The induced drag is zero at zero lift.

40.13 FLOW MEASUREMENTS

Fluid flow measurements generally involve determining static pressures, local and average velocities, and volumetric or mass flow rates.

40.13.1 Pressure Measurements

Static pressures are measured by means of a small hole in a boundary surface connected to a sensor—a manometer, a mechanical pressure gage, or an electrical transducer. The surface may be a duct wall or the outer surface of a tube, such as those shown in Fig. 40.38. In any case, the surface past which the fluid flows must be smooth, and the tapped holes must be at right angles to the surface.

Table 40.12 Drag Coefficients for Three-Dimensional Shapes Re between 10^4 and 10^6 (Flow is from Left to Right)

Shape		C_D
Disk	|	1.17
Open hemisphere	(	0.38
	)	1.42
Solid hemisphere	◖	0.42
	◗	1.17
Cube	□	1.05[a]
	◇	0.80[a]
Cone, 60°	<	0.50

[a]Mounted on a boundary wall.

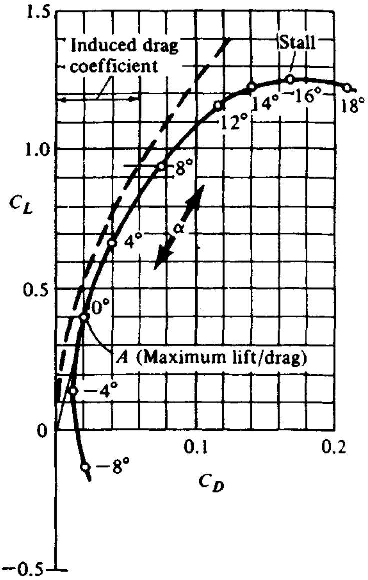

Fig. 40.37 Typical polar diagram showing lift–drag characteristics for an airfoil of finite span.

Total or stagnation pressures are easily measured accurately with an open-ended tube facing into the flow, as shown in Fig. 40.38.

40.13.2 Velocity Measurements

A combined pitot tube (Fig. 40.38) measures or detects the difference between the total or stagnation pressure p_0 and the static pressure p. For an incompressible fluid the velocity being measured is $V = \sqrt{2(p_0 - p)/\rho}$. For subsonic gas flow the velocity of a stream at a temperature T and pressure p in

$$V = \sqrt{\frac{2kRT}{k-1}\left[\left(\frac{p_0}{p}\right)^{(k-1)/k} - 1\right]}$$

and the corresponding Mach number is

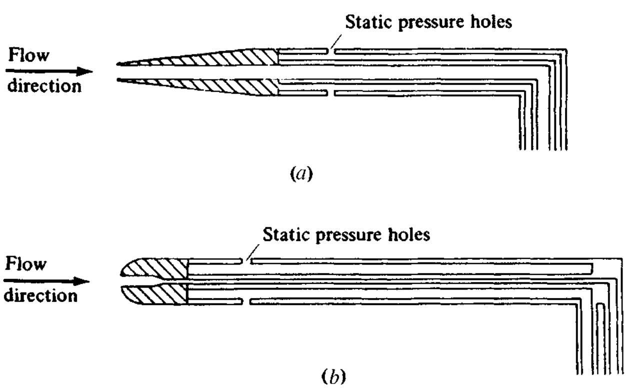

Fig. 40.38 Combined pitot tubes: (a) Brabbee's design; (b) Prandtl's design—accurate over a greater range of yaw angles.

$$M = \sqrt{\frac{2}{k-1}\left[\left(\frac{p_0}{p}\right)^{(k-1)/k} - 1\right]}$$

For supersonic flow the stagnation pressure p_{0y} is downstream of a shock, which is detached and ahead of the open stagnation tube, and the static pressure p_x is upstream of the shock. In a wind tunnel the static pressure could be measured with a pressure tap in the tunnel wall. The Mach number M of the flow is

$$\frac{p_{0y}}{p} = \left(\frac{k+1}{2}M^2\right)^{k/(k-1)}\left(\frac{2k}{k+1}M^2 - \frac{k-1}{k+1}\right)^{1/(1-k)}$$

which is tabulated in gas tables.

In a mixture of gas bubbles and a liquid for gas concentrations C no more than 0.6 by volume, the velocity of the mixture with the pitot tube and manometer free of bubbles is

$$V_{\text{mixture}} = \sqrt{\frac{2(p_0 - p_1)}{(1-C)\rho_{\text{liquid}}}} = \sqrt{\frac{2gh_m}{(1-C)}\left(\frac{\gamma_m}{\gamma_{\text{liquid}}} - 1\right)}$$

where h_m is the manometer deflection in meters for a manometer liquid of specific weight γ_m. The error in this equation from neglecting compressible effects for the gas bubbles is shown in Fig. 40.39. A more correct equation based on the gas–liquid mixture reaching a stagnation pressure isentropically is

$$\frac{V_1^2}{2} = \frac{p_0 - p_1}{\rho_u(1-C)} + \frac{C}{1-C}\left(\frac{p_1}{\rho_u}\right)\left[\frac{k}{k-1}\left(\frac{p_0}{p_1}\right)^{(k-1)/k} - \frac{1}{k-1} - \left(\frac{p_0}{p_1}\right)\right]$$

but is cumbersome to use. As indicated in Fig. 40.39 the error in using the first equation is very small for high concentrations of gas bubbles at low speeds and for low concentrations at high speeds.

If n velocity readings are taken at the centroid of n subareas in a duct, the average velocity V from the point velocity readings u_i is

$$V = \frac{1}{n}\sum_{i=1}^{n} u_i$$

In a circular duct, readings should be taken at $(r/R)^2 = 0.055, 0.15, 0.25, \ldots, 0.95$. Velocities measured at other radial positions may be plotted versus $(r/R)^2$, and the area under the curve may be integrated numerically to obtain the average velocity.

Other methods of measuring fluid velocities include length–time measurements with floats or neutral-buoyancy particles, rotating instruments such as anemometers and current meters, hot-wire and hot-film anemometers, and laser-doppler anemometers.

40.13.3 Volumetric and Mass Flow Fluid Measurements

Liquid flow rates in pipes are commonly measured with commercial water meters; with rotameters; and with venturi, nozzle, and orifice meters. These latter types provide an obstruction in the flow and make use of the resulting pressure change to indicate the flow rate.

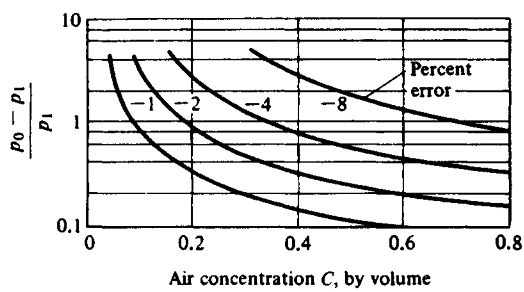

Fig. 40.39 Error in neglecting compressibility of air in measuring velocity of air–water mixture with a combined pitot tube.

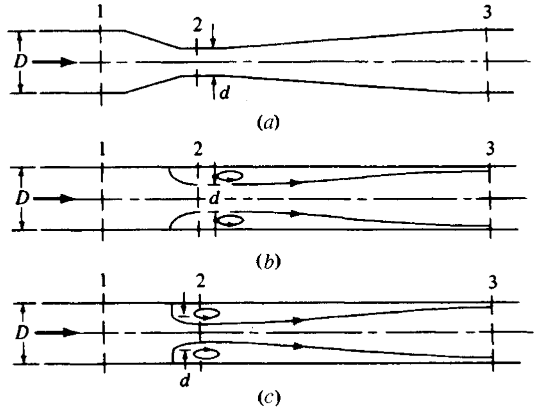

Fig. 40.40 Pipe flow meters: (*a*) venturi; (*b*) nozzle; (c) concentric orifice.

The continuity and Bernoulli equations for liquid flow applied between sections 1 and 2 in Fig. 40.40 give the ideal volumetric flow rate as

$$Q_{\text{ideal}} = \frac{A_2\sqrt{2g\,\Delta h}}{\sqrt{1 - (A_2/A_1)^2}}$$

where Δh is the change in piezometric head. A form of this equation generally used is

$$Q = K\left(\frac{\pi d^2}{4}\right)\sqrt{2g\,\Delta h}$$

where K is the flow coefficient, which depends on the type of meter, the diameter ratio d/D, and the viscous effects given in terms of the Reynolds number. This is based on the length parameter d and the velocity V through the hole of diameter d. Approximate flow coefficients are given in Fig. 40.41. The relation between the flow coefficient K and this Reynolds number is

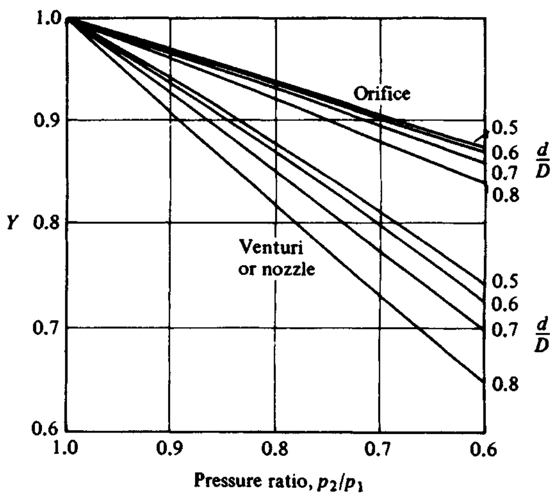

Fig. 40.41 Approximate flow coefficients for pipe meters.

$$\mathrm{Re}_d = \frac{Vd}{v} = \frac{Qd}{\frac{1}{4}\pi d^2 v} = K\frac{d\sqrt{2g\,\Delta h}}{v}$$

The dimensionless parameter $d\sqrt{2g\,\Delta h}/v$ can be calculated, and the intersection of the appropriate line for this parameter and the appropriate meter curve gives an approximation to the flow coefficient K. The lower values of K for the orifice result from the contraction of the jet beyond the orifice where pressure taps may be located. Meter throat pressures should not be so low as to create cavitation. Meters should be calibrated in place or purchased from a manufacturer and installed according to instructions.

Elbow meters may be calibrated in place to serve as metering devices, by measuring the difference in pressure between the inner and outer radii of the elbow as a function of flow rate.

For compressible gas flows, isentropic flow is assumed for flow between sections 1 and 2 in Fig. 40.40. The mass flow rate is $\dot{m} = KYA_2\sqrt{2\rho_1(p_1 - p_2)}$, where K is as shown in Fig. 40.41 and $Y = Y(k, p_2/p_1, d/D)$ and is the expansion factor shown in Fig. 40.42. For nozzles and venturi tubes

$$Y = \sqrt{\frac{\left(\dfrac{k}{k-1}\right)\left(\dfrac{p_2}{p_1}\right)^{2/k}\left[1 - \left(\dfrac{p_2}{p_1}\right)^{(k-1)/k}\right]\left[1 - \left(\dfrac{d}{D}\right)^4\right]}{\left[1 - \left(\dfrac{p_2}{p_1}\right)\right]\left[1 - \left(\dfrac{d}{D}\right)^4\left(\dfrac{p_2}{p_1}\right)^{2/k}\right]}}$$

and for orifice meters

$$Y = 1 - \frac{1}{k}\left[0.41 + 0.35\left(\frac{d}{D}\right)^4\right]\left(1 - \frac{p_2}{p_1}\right)$$

These are the basic principles of fluid flow measurements. Utmost care must be taken when accurate measurements are necessary, and reference to meter manufacturers' pamphlets or measurements handbooks should be made.

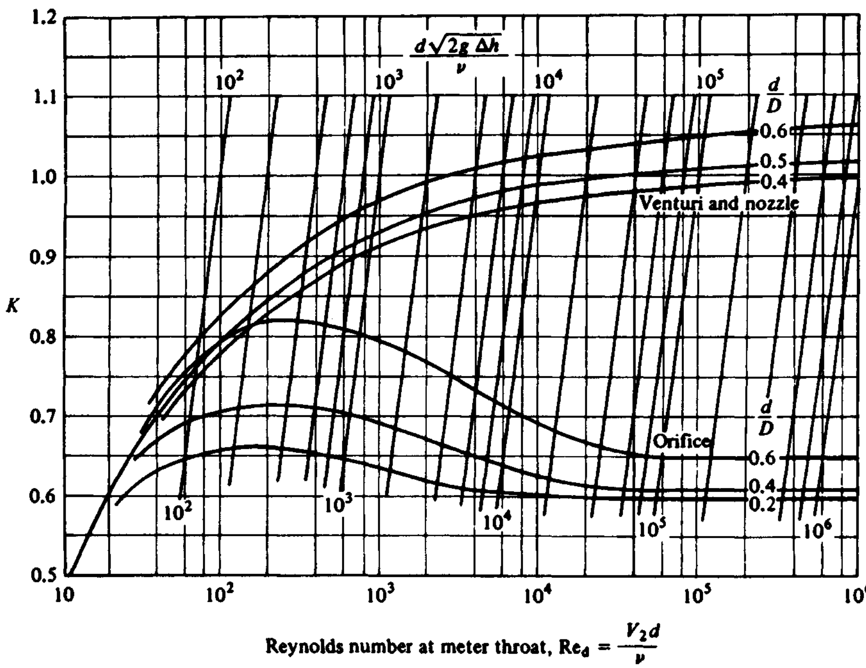

Fig. 40.42 Expansion factors for pipe meters, $k = 1.4$.

BIBLIOGRAPHY

General

Olson, R. M., *Essentials of Engineering Fluid Mechanics,* 4th ed., Harper and Row, New York, 1980.

Streeter, V. L. (ed.), *Handbook of Fluid Dynamics,* McGraw-Hill, New York, 1961.

Streeter, V. L., and E. B. Wylie, *Fluid Mechanics,* McGraw-Hill, New York, 1979.

Section 40.9

Schlichting, H., *Boundary Layer Theory* (translated by J. Kestin), 7th ed., McGraw-Hill, New York, 1979.

Section 40.10

Shapiro, A. H., *The Dynamics and Thermodynamics of Compressible Fluid Flow,* Ronald Press, New York, 1953, Vol. I.

Section 40.12

Hoerner, S. F., *Fluid-Dynamic Drag,* S. F. Hoerner, Midland Park, NJ, 1958.

Section 40.13

Miller, R. W., *Flow Measurement Engineering Handbook,* McGraw-Hill, New York, 1983.

Ower, E., and R. C. Pankhurst, *Measurement of Air Flow,* Pergamon Press, Elmsford, NY, 1977.